9 Functional Magnetic Resonance Imaging

Peter A. Bandettini

The idea of using magnetic resonance imaging (MRI) to assess human brain activation noninvasively, rapidly, and with relatively high spatial resolution, was, before 1990, pure fantasy. The arrival of functional MRI (fMRI) was marked by the publication of the groundbreaking paper by Belliveau et al. (1991) in November of 1991. Although innovative and generating considerable excitement, the "Belliveau technique," which involved two bolus injections of gadolinium-DTPA to characterize blood volume changes with activation, was effectively made obsolete as a brain activation assessment method by the time it was published. It was replaced by a completely noninvasive MRI-based technique using endogenous functional contrast associated with localized changes in blood oxygenation during activation.

Between the late spring and early fall of 1991, the first successful experiments were carried out at the Massachusetts General Hospital (May), University of Minnesota (June), and Medical College of Wisconsin (September) using endogenous MRI contrast to assess brain activation. These experiments were published within two weeks of each other in the early summer of 1992.

The mechanism of endogenous contrast on which the activation assessments were based was pioneered by Ogawa et al. (1990), who coined the term *blood oxygenation level–dependent* (BOLD), and by Turner et al. (1991), who discovered the contrast while searching for changes in the diffusion coefficient among apnea patients. In a prescient comment in 1990—two years before the first successful experiments were published and about a year before the first successful experiments were performed—Ogawa et al. (1990) predicted the beginning of a new method to assess brain activation.

A still earlier brain study using positron-emission tomography (PET; Fox and Raichle, 1986) had demonstrated an activation-induced decrease

in the oxygen extraction fraction, thus predicting an increase in the MRI signal with activation. And, indeed, as researchers would find, the BOLD fMRI signal did increase with an increase in brain activation.

Another noninvasive fMRI technique, emerging almost simultaneously with BOLD fMRI, is known as "arterial spin labeling" (ASL; Williams et al., 1992). The contrast in ASL arises from cerebral blood flow and perfusion, independent of blood oxygenation. Other techniques, allowing noninvasive assessment of activation-induced changes in cerebral blood volume (Lu et al., 2003) and oxidative metabolic rate (Davis et al., 1998; Hoge et al., 1999) have since been developed.

BOLD fMRI is currently the brain activation–mapping method of choice for almost all neuroscientists because it is easiest to implement and the functional contrast to noise is 2 to 4 times higher than the other methods. Functional contrast to noise (defined as the ratio of signal change to background fluctuations) ranges from 2 to about 6 at higher field strengths when BOLD contrast is used. Currently, the need for sensitivity outweighs the need for specificity, stability over long periods of time, quantitation, or baseline state information—all of which are advantages inherent to ASL, and all of which come at the price of sensitivity.

Since these first discoveries, hardware, methodology, signal interpretability, and applications have been advancing synergistically. Advances in hardware include scanners with increased magnetic field strength, improved radiofrequency coils, and subject interface devices; those in methodology include pulse sequences, postprocessing, multimodal integration, and improved paradigm design. Advances in signal interpretability include improved understanding of the relationship between underlying neuronal activity, on the one hand, and simultaneous direct measures of neuronal activity and precise modulation of its dynamics and magnitudes obtained through use of BOLD fMRI, on the other; in applications, advances have been directed both at understanding brain organization and at complementing clinical diagnoses and characterizing neurological and psychiatric disorders. Generally, advances in any one of these domains have furthered advances in the others; the needs of one domain have in many instances driven the development of the others. (This exciting, highly interdisciplinary coevolution is described in the "Development" section.)

Even though fMRI is nearly 15 years old, unknowns remain regarding the physiological and biophysical factors influencing fMRI signal changes. New insights into the principles of BOLD and other fMRI contrast mechanisms as well as image acquisition and postprocessing are published at a steady rate. (The latest information regarding the acquisition,

processing, and interpretation of fMRI signal changes is presented in the "Principles" section.)

Functional MRI is continually being shaped by innovations in hardware, methodology, interpretation, and applications. Scanner field strength and image acquisitions hardware grow ever more sophisticated—allowing greater sensitivity, speed of acquisition, and resolution. Paradigm design and postprocessing methods continually evolve as applications demand. New methods for integrating fMRI with other brain activation assessment techniques have emerged, allowing more precise interpretation of fMRI signal changes and introducing novel applications. Although most fMRI applications remain in the research domain, with continuing improvements in robustness and interpretability, especially in regard to activation maps and signal change dynamics of specific patient populations, fMRI is poised to make a clinical impact as well. (All these topics are covered, and highlights of fMRI development described, in the "Development" section.)

That the sources of contrast in functional MRI—cerebral blood flow, volume, and oxygenation changes—are secondary to brain activation places an inherent limitation on the upper spatial and temporal resolution and on the interpretability of the technique. Other fMRI limitations include sensitivity to subject motion, signal dropout in specific regions, and temporal instability within and across scanning sessions. (These limitations are described, and to overcome them outlined, methods in the "Limitations" section.)

The scope and success of the best fMRI research and applications are defined by how well the paradigms, processing, and interpretation of results are integrated with other brain function assessment techniques. This integration has yielded far greater insights into human brain function than any that fMRI could provide on its own. Techniques successfully integrated with fMRI include behavioral measures, electroencephalography (EEG), magnetoencephalography (MEG), physiological measurements, optical imaging, electrophysiological measurements, and transcranial magnetic stimulation (TMS). (The basics of how these techniques are used in conjunction with fMRI, and of the insights gained, are presented in the "Integration" section.)

Development

It is important first to put fMRI development in context. In 1991, brain activation studies were being performed by a handful of groups using techniques involving ionizing radiation or electroencephalography. Although

these techniques are still quite useful today, providing complementary information, functional MRI, as it came into common use in the early nineties, represented a huge leap in ease and flexibility of brain-mapping experimentation. After 1992, investigators undertaking brain activation studies had simply to put their subjects in the scanner, have them perform a task during time series image collection, and look for MRI changes. This proved to be both a blessing and a curse for the burgeoning brain-mapping community.

On the "curse" side, easy access to this powerful tool has given rise to many poorly planned, executed, and analyzed experiments filled with overinterpretation of artifactual signal changes (although fewer today, with rapid improvements in the collective expertise of the imaging community). Moreover, the frantic rush to pick the scientific "low-hanging fruit" that began in earnest with the introduction of functional imaging continues in many contexts today. Most fMRI researchers, myself included, have been caught up in the exciting sense of urgency to use this extraordinarily powerful technique, whose potential we have only glimpsed.

On the "blessing" side, however, fMRI has brought unique insights into how the human brain is organized, how it changes over time (from seconds to years) and varies across populations, and has steadily advanced our understanding of human cognition. Most important, it has given rise to a much larger collective effort toward using brain-mapping technology for research—and to the start of an effort toward applying fMRI to diagnose and treat clinical populations.

Circa 1992, only a handful of laboratories could perform fMRI: it required not only an MRI scanner but also the capability of performing high-speed MRI—known as "echo planar imaging" (EPI). With EPI, neuroimagers could collect an entire image (or "plane") with the use of a single radio frequency (RF) pulse and subsequent signal "echo," hence the name "echo planar." Typical clinical MRI sequences use at least 128 RF pulses for a single image. One pulse typically yields a "line" of data. To collect an image with one RF pulse requires that the imaging gradients (used to spatially encode the data and thus to create an image) be oscillated very rapidly since the usable signal only lasts for about 100 msec. Because a waiting period is required between RF pulses, called the "repetition time" (TR—typically 100 msec to 2 sec), and also because clinical images typically have at least 128 lines, such an image takes on the order of several seconds to several minutes to collect. An important point is that not only do clinical images take time, but because of signal fluctuations with repeated collection of the same image, their temporal stability is relatively low, with cardiac

and respiratory effects producing nonrepeatable image artifacts. Collecting an entire image in 30 msec with EPI, however, "freezes" these physiological processes, causing artifacts to be more or less precisely replicated from image to image over time (with some exceptions)—thus substantially increasing temporal stability. It should be noted that, although some early studies adopted artifact correction strategies that used non-EPI techniques, using EPI and, more generally, "single-shot" techniques using one RF pulse per image is the most common and successful strategy. Hardware for performing EPI was not available on clinical systems until about 1996. Before that time, centers that performed EPI made use of low-inductance gradient coils built in-house or, if they were fortunate enough collaborated with small companies whose systems, also built in-house, allowed rapid gradient switching. Hardware availability remains an issue to this day. The most innovative technology for performing fMRI is at least several years ahead of what is available on clinical scanners. Because functional MRI remains a nonclinical technique, vendors simply choose to apply their research and development efforts elsewhere. This is certain to change when fMRI's clinical utility becomes more apparent.

Figure 9.1 shows the results of a science citation index reference search on fMRI-related papers published since 1992. The number of papers published appears to grow exponentially until 2001, before dropping into a steep, but arching second phase of growth from 2002 on. Papers published before 1996 were typically performed on systems developed in-house. After 1996, the number of groups performing fMRI expanded rapidly. To add a dimension of perspective to this plot, table 9.1 shows a list of the fifty most

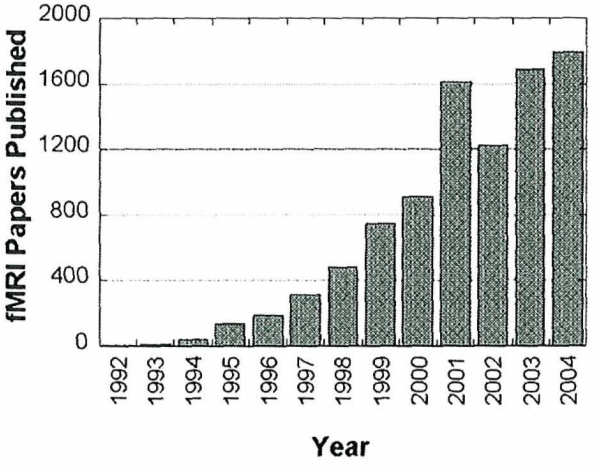

Figure 9.1
Bar graph of the approximate number of fMRI papers published, as determined by a Medline search for the keywords "fMRI" or "functional MRI" after 1993.

Table 9.1
Fifty most frequently cited papers on functional MRI (as of December 2004)

Rank	Citations per Year	Total Citations	Authors	Type
1	114	1485	Kwong et al., 1992	M
2	112	448	Logothetis et al., 2001	I
3	101	507	Cabeza and Nyberg, 2000	A
4	84	1095	Ogawa et al., 1992	M
5	82	655	Kanwisher et al., 1997	A
6	71	857	Bandettini et al., 1993	M
7	67	336	Bush et al., 2000	A
8	60	419	Carter et al., 1998	A
9	58	231	Egan et al., 2001	A
10	57	458	Cohen et al., 1997	M/A
11	57	509	Cox, 1996	M
12	55	497	Martin et al., 1996	A
13	53	745	Belliveau et al., 1991	M
14	53	691	Bandettini et al., 1992	M
15	52	523	Sereno et al., 1995	M/A
16	50	348	Wagner et al., 1998	A
17	50	348	Whalen et al., 1998	A
18	48	428	Worsley et al., 1996	M
19	47	233	Corbetta et al., 2000	A
20	44	174	O'Doherty et al., 2001	A
21	44	87	Egan et al., 2003	A
22	43	173	Fletcher and Henson, 2001	A
23	43	427	Tootell et al., 1995	M/A
24	42	419	Shaywitz et al., 1995	A
25	42	418	Worsley and Friston, 1995	M
26	41	446	Pellerin and Magistretti, 1994	I
27	40	359	Breiter et al., 1996	A
28	40	319	Binder et al., 1997	A
29	40	317	Braver et al., 1997	M/A
30	39	393	D'Esposito et al., 1995	A
31	39	391	Friston et al., 1995	M
32	39	348	Boynton et al., 1996	I
33	39	348	Malonek and Grinvald, 1996	I/A
34	38	384	Karni et al., 1995	A
35	38	114	Corbetta and Shulman, 2002	A
36	38	455	Ogawa et al., 1993	I
37	38	303	Courtney et al., 1997	M/A
38	37	185	Haxby et al., 2000	A

Table 9.1
(continued)

Rank	Citations per Year	Total Citations	Authors	Type
39	37	443	Rao et al., 1993	A
40	37	368	Buckner et al., 1995	A
41	37	365	Forman et al., 1995	M
42	36	181	Hopfinger et al., 2000	A
43	36	253	Kelley et al., 1998	A
44	36	249	Corbetta et al., 1998	A
45	35	317	Courtney et al., 1996	A
46	34	344	Demb et al., 1995	A
47	34	271	Dale and Buckner, 1997	M
48	34	203	Friston et al., 1999	M
49	33	200	Botvinick et al., 1999	A
50	33	231	Courtney et al., 1998	A

Based on science citation search of "fMRI" or "functional MRI." "A" papers focus on application of FMRI toward a specific neuroscience or clinical question; "M," papers on methods development; and "I" papers, on the relationship between neuronal activity and fMRI signal changes; some papers are combinations of these types. See reference list for full publication information.

frequently cited fMRI papers since 1991. It is worth noting that many of the studies labeled "M/A," indicating that they specifically employed fMRI to derive a novel insight into brain organization, were carried out by neuroscientists who have worked closely with individuals in methodology development. This serves to highlight the multidisciplinary nature of fMRI and the fact that many cutting-edge applications are still closely tied to advances in methodology. It is also worth noting, however, that, since the title search keywords were simply "fMRI" or "functional MRI," many relevant papers were likely missed.

After about 1996, with the rapid proliferation of EPI-capable MRI scanners incorporating whole-body gradients, functional magnetic resonance imaging arrived at the operating platform that is still "standard" today—sequence: gradient-echo EPI; echo time (TE): 40 msec; matrix size: 64×64; field of view: 24 cm; slice thickness: 4 mm. Typically, whole-brain volume coverage is achieved using a repetition time (TR) of 2 seconds, with time series lasting on the order of 5 to 8 minutes and with about 7 time series collected per subject-scanning session. Multisubject studies usually settle on assessing about 12 such sessions. And typically, a whole-brain,

single quadrature RF coil is used; around 2002, the "standard" field strength was increased from 1.5 T to 3 T.

Beyond basic collection, standards begin to diverge; paradigm design and postprocessing are still evolving steadily. Nevertheless, "typical" paradigm design methods are either "boxcar," involving steady-state activation periods of 10 seconds or more, or more commonly, "event-related" designs, enjoying the flexibility inherent to brief activation periods interspersed within a given time series. For processing, SPM is the most common software, followed closely by software platforms such as Brain Voyager, FSL, and AFNI. The most common techniques use "reference" functions for statistical map creation; when multisubject data are involved, statistical maps are spatially smoothed and transformed to a standardized space for comparison or averaging. Recent technological advances have made possible the unprecedented visualization and navigation of fMRI data (see figure 9.2, plate 3).

Figure 9.2
Example of how the same fMRI data in their various forms can be simultaneously and interactively visualized. Data are from a retinotopy experiment (expanding ring); processing and visualization were performed using AFNI and SUMA (Cox, 1996) and surface models created with FreeSurfer (Dale, Fischl, and Sereno, 1999). Central panel shows AFNI's main controller window used to select and control data to be visualized. (*A*) Echo planar imaging (EPI) time series from voxels in the occipital cortex during cyclic visual stimulation. Of the 9 voxels shown here, some show clear modulation at the main frequency of the stimulus; others do not. (*B*) Statistical maps in color overlaid atop high-resolution anatomical data. The colored voxels represent response delay of significantly activated voxels and the cross hair represents the location of the central voxel in (*A*). Contours of pial and white matter/gray matter boundary surface models are shown in blue and red lines. (*C*) Three-dimensional volume rendering of the data shown in panel B with cutouts revealing the calcarine sulcus. (*D*) Functional imaging data projected on models of the same cortical surface with varying degrees of deformation. From left to right we have the white matter/gray matter boundary surface, an inflated version that reveals buried portions of sulci, a spherical version that can be warped into a standard coordinate space for surface-based group analysis (Fischl et al., 1999; Van Essen and Drury, 1997; Saad et al., 2004) and a flattened version of the occipital cortex with the data represented in color and relief form. Note that all panels were created simultaneously and interactively. For example, a change of statistical threshold in the main AFNI controller, will affect all displays in panels (*B*) through (*D*). A selection of a new location on the flat map in (*D*) will cause all other viewers to jump to the corresponding new location. (Figure and caption provided courtesy of Ziad Saad, Ph.D., Statistical and Scientific Computing Core Facility, National Institute of Mental Health) See plate 3 for color version.

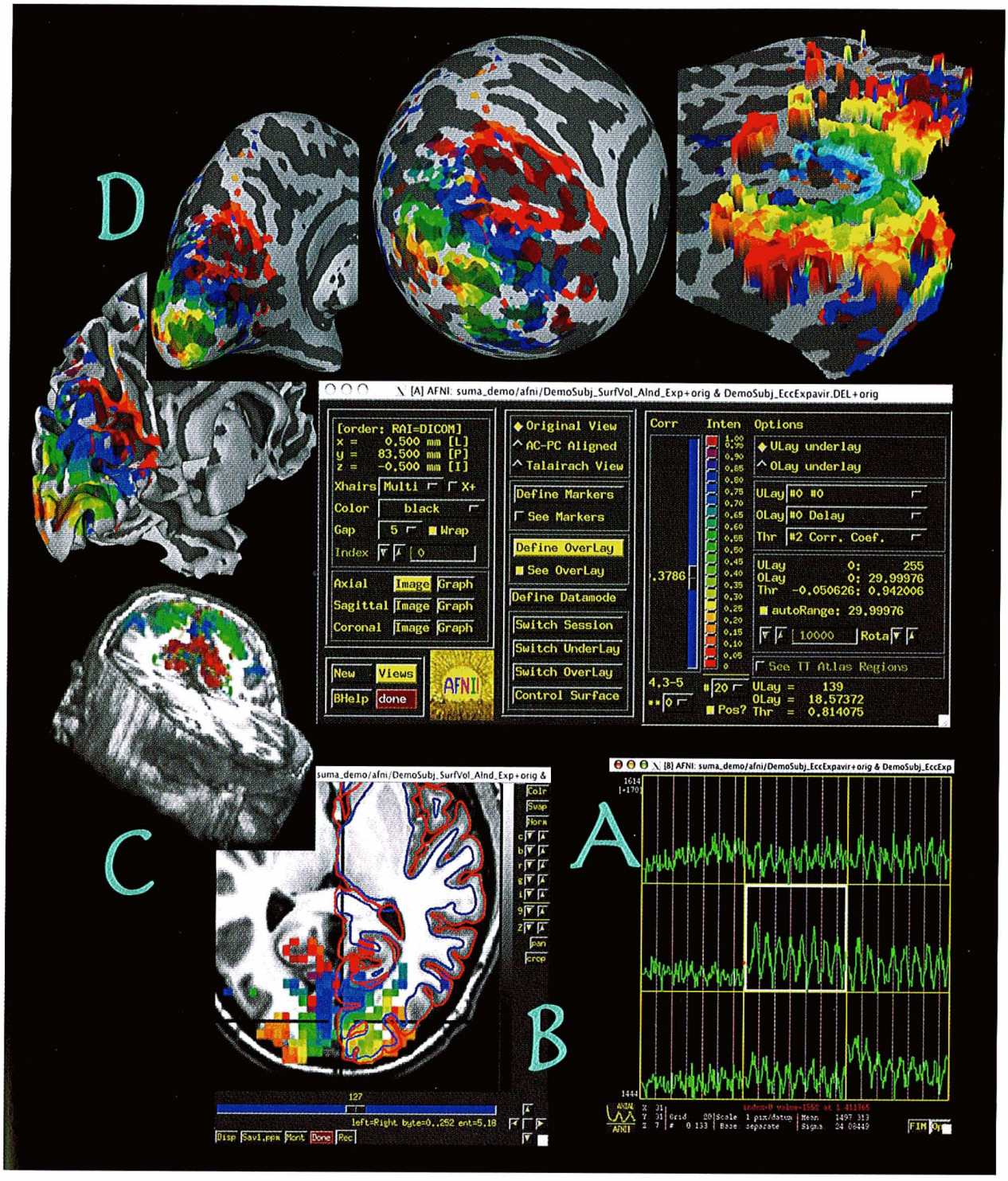

Plate 3

Example of how the same fMRI data, in their various forms, can be simultaneously and interactively visualized. See body of text for figure legend.

Overall, the evolution of fMRI has been punctuated by novel techniques, findings, and controversies. For a sense of perspective, here are just eleven of the more prominent developments in fMRI before 2003:

- Parametric manipulation of brain activation demonstrates that BOLD contrast roughly follows the level of brain activation in the visual system (Kwong et al., 1992), the auditory system (Binder et al., 1994), and the motor system (Rao et al., 1996).
- Event-related fMRI is first demonstrated (Blamire et al., 1992), then applied to cognitive activation (Buckner et al., 1996; McCarthy et al., 1997). Mixed event-related and block designs are developed (Visscher et al., 2003); paradigms are demonstrated in which the activation timing of multiple brain systems timing was orthogonal, allowing multiple conditions to be cleanly extracted from a single run (Courtney et al., 1997).
- High-resolution maps are created for spatial resolution in ocular dominance columns (Menon et al., 1997; Cheng, Waggoner, and Tanaka, 2001); activation maps are created for cortical layers (Logothetis et al., 2002). Extraction of information at high spatial frequencies within regions of activation is demonstrated (Haxby et al., 2001); timings from one to hundreds of milliseconds are extracted for temporal resolution (Ogawa et al., 2000; Menon, Luknowsky, and Gati, 1998; Henson et al., 2002; Bellgowan, Saad, and Bandettini, 2003).
- "Deconvolution" methods are developed for rapid presentation of stimuli (Dale and Buckner, 1997).
- Early BOLD contrast models (Ogawa et al., 1993; Buxton and Frank, 1997), are followed by more sophisticated models that more fully integrate the latest data on hemodynamic and metabolic changes (Buxton et al., 2004).
- Continuous variation of visual stimuli parameters as a function of time is proven to be a powerful method for fMRI-based retinotopy (Engel et al., 1994; DeYoe et al., 1994; Sereno et al., 1995).
- "Clustered-volume" acquisition is developed to avoid scanner noise artifacts (Edmister et al., 1999).
- Functionally related resting states are correlated (Biswal et al., 1995) and regions consistently showing deactivation described (Binder et al., 1999; Raichle et al., 2001).
- The "pre-undershoot" in fMRI is observed (Hennig et al., 1997; Menon, Ogawa, and Ugurbil, 1995; Hu, Le, and Ugurbil, 1997) and correlated with optical imaging (Malonek and Grinvald, 1996).
- Simultaneous use of fMRI and direct electrophysiological recording in nonhuman primate brain during visual stimulation elucidates the rela-

tionship between fMRI and BOLD fMRI contrast (Logothetis et al., 2001). Simultaneous electrophysiological recordings in animal models reveal a correlation between negative signal changes and decreased neuronal activity (Shmuel et al., 2002). Simultaneous electrophysiological recordings in animal models provide evidence that inhibitory input can cause an increase in cerebral blood flow (Mathiesen et al., 1998).

- Structural equation modeling is developed for fMRI time series analysis (Buchel and Friston, 1998).

This list is only a sampling of the tremendous number of novel developments that have established fMRI as a powerful tool for investigating and quantitating human brain activity.

Principles

With functional magnetic resonance imaging, neuroimagers are able to map the following types of physiological information: baseline cerebral blood volume (Rosen et al., 1991), changes in cerebral blood volume (Belliveau et al., 1991; Lu et al., 2003), quantitative measures of baseline and changes in cerebral perfusion (Wong et al., 1999), changes in cerebral blood oxygenation (Bandettini et al., 1992; Blamire et al., 1992; Frahm et al., 1992; Kwong et al., 1992, Ogawa et al., 1992), the resting-state cerebral oxygen extraction fraction (An et al., 2001), and changes in the cerebral metabolic rate for oxygen ($CMRO_2$) (Davis et al., 1998; Hoge et al., 1999).

BOLD Contrast

Let us consider first the basic mechanism for BOLD fMRI signal changes with brain activation. In brain tissue during resting state, blood oxygenation in capillaries and veins is lower than that of arteries due to the extraction of oxygen from the blood. Deoxyhemoglobin (deoxy-Hb) has a different susceptibility from surrounding brain tissue and water, whereas oxyhemoglobin (oxy-Hb) has the same susceptibility. An object, a deoxy-Hb molecule, say, or a capillary or vein containing deoxy-Hb molecules, that has a different susceptibility from its surrounding tissue creates a magnetic field distortion when placed in a magnetic field. Water molecules (the primary signal source in MRI), also called "spins," precess at a frequency that is directly proportional to the magnetic field they are experiencing. Within a voxel, if spins are precessing at different frequencies, they rapidly become out of phase. The strength of the MRI signal is directly proportional to the coherence of spins: when they are completely out of phase,

destructive addition takes place and there is no signal; when they are completely in phase, there is maximal signal. During resting state, enough spins are out of phase, due to the many microscopic field distortions in each voxel, to cause the MRI signal to be attenuated somewhat relative to when there is no deoxy-Hb present.

By contrast, and for reasons not fully understood, during activation, cerebral blood flow increases locally such that there is an overabundance of oxygenated blood delivered to the active regions. This causes the amount of deoxy-Hb, and thus also the magnitude of the magnetic field distortions, to decrease, which increases the coherence of spins within each voxel and leads to an MRI signal increase of a few percent.

The signal begins to increase approximately 2 seconds after neuronal activity begins, and plateaus in the "on" state after about 7 to 10 seconds. Although a "pre-undershoot" is sometimes observed, a "post-undershoot" is more commonly observed. These effects are likely due to transient mismatches between either cerebral blood volume or the cerebral metabolic rate for oxygen ($CMRO_2$) before and after respective increases and decreases in blood flow occur. The dynamics, location, and magnitude of the MRI signal are highly influenced by the vasculature in each voxel. If voxels happen to capture large vessel effects, the magnitude of the signal may be large (up to an order of magnitude greater than that for capillary effects), the timing somewhat more delayed than average (up to 4 seconds more delayed than for capillary effects), and the location of the signal somewhat distal (up to a centimeter) from the true region of activation. Although improvements in methodology have minimized the effects of this variability, the problem of variable vasculature and hemodynamic coupling nevertheless remains at all field strengths in fMRI, limiting the depth and range of questions that can be addressed using this technique.

Perfusion Contrast

Introduced at almost the same time as BOLD functional MRI was the noninvasive method for mapping perfusion in the human brain known as "arterial spin labeling" (ASL). The technique generally involves applying a radio frequency pulse (or continuous RF excitation) below the imaging plane (in the neck area). Without blood flow, the magnetization applied to brain tissue would simply decay and not influence the MRI signal where the images were being collected. With blood flow, however, the altered magnetization of the "labeled" blood affects the longitudinal magnetization (T1) in the imaging slices as it flows, and as water spins mix and exchange mag-

netization, in the imaged brain tissue. A second set of images is obtained either with the label applied above the brain or not applied at all. Therefore these second images are not affected in the same manner by magnetization of inflowing spins. The last step is to perform pairwise subtraction on the two sets of images, removing all the anatomical signal from each image pair, leaving behind only the effect on the signal by the label. Because of the low signal to noise inherent to this type of contrast, an average of typically several hundred "label-minus-no-label" pairs are obtained to create a map of baseline perfusion.

A strong determinant of perfusion contrast with the ASL technique is the time between the labeling pulse and the subsequent image collection, designated as "TI." If the TI is 200 msec, only the effects of the most rapidly flowing blood can be observed (typically, in arteries). As the TI approaches 1 second, slower perfusing spins in and around capillaries appear. Above 1 second, the magnetization of the label decays significantly. A time series of these "label-minus-no-label" pairs can be collected for the purpose of functional imaging of brain activation. Arterial spin labeling has not achieved the success of BOLD functional MRI mostly because of limitations in the number of slices obtainable, temporal resolution, and decreased functional contrast to noise of the technique relative to BOLD fMRI. Nevertheless, the superior functional specificity and stability of arterial spin labeling over long periods of time, along with its quantitative information, have made it useful for many applications where BOLD fMRI falls short.

Sensitivity

A primary struggle in fMRI is to increase sensitivity. This is achieved by increasing the magnitude of the signal change or by decreasing the effects of noise. This struggle has also been the impetus for imaging at ever higher field strengths. With an increase in field strength, signal to noise increases proportionally and both BOLD and perfusion contrast increase—BOLD contrast increasing with greater changes in transverse relaxation relative to activation, and perfusion contrast increasing with increases in the T1 of blood, which allows the magnetization of the labeled blood to remain longer. Aside from system instabilities, however, higher field strengths result in generally poorer images at the base of the brain due to greater effects of poor shimming and to greater physiological fluctuations. Methods for removing these fluctuations remain imperfect. That said, a primary advantage of imaging at higher field strengths (e.g., 7 T) is that the lower limit of signal to noise is achieved with a much smaller voxel volume, thus

allowing much higher imaging resolution (down to $1\,mm^3$) at functional contrast levels comparable to those of imaging at 3 T with voxel volumes of $3\,mm^3$. This increase in resolution without prohibitive losses in sensitivity may explain why imaging of ocular dominance column activation has been successful at 4 T but not at lower field strengths. Currently, successful results in imaging humans have been obtained at 7 T (Vaughan et al., 2001; Pfeuffer et al., 2002b; Yacoub et al., 2001); such results are certain to multiply rapidly.

Other processing steps for increasing sensitivity include temporal and spatial smoothing. Because of the inherent temporal autocorrelation in the signal from hemodynamics or other physiological processes, temporal smoothing is performed so that the temporal degrees of freedom may be accurately assessed. Spatial smoothing can be performed if high spatial frequency information is not desired and as a necessary prespatial normalization step (matching effective resolution with the degree of variability associated with spatial normalization techniques) for multisubject averaging and comparison. An often overlooked fact is that higher temporal sensitivity with less image warping due to a shorter readout window is achieved, not by spatially smoothing the maps after data collection, but by collecting the images at the desired spatial resolution in the first place. Indeed, in many instances, spatial smoothing is clearly *not* desired—particularly when high spatial frequency information in individual maps is compared (Haxby et al., 2001).

Once images are collected, and after motion correction is performed, a time series analysis is carried out voxel by voxel. Typically, a model function or functions are used as regressors, and the significance of the correlation of the time series data with the regressors calculated, again voxel by voxel. If the expected activation timing is not known, a more open-ended approach to analysis is taken, such as independent component analysis (Beckmann and Smith, 2004).

Innovation

The quantity and impact of innovations, and the proportion of truly high quality work, in functional magnetic resonance imaging have continued to grow as the field has matured, making it nearly impossible to stay abreast of the latest and the most interesting advances. Whereas the "Development" section touched on major, "established" innovations of the past 14 years, to give a sense of the vibrancy of the fMRI field, and of its potential for

expanding in ever new, exciting directions, this section will highlight emerging innovations that may or may not pan out and make a major impact.

Imaging Technology

Recent innovations in acquisition hardware and imaging strategy may take functional magnetic resonance imaging to new levels of sensitivity, resolution, and speed. Typical acquisition hardware uses a single-quadrature, whole-brain RF coil feeding into one acquisition channel, and collects single-shot echo planar imaging data at 64 × 64 resolution. Recently, the ability to acquire MRI data with simultaneous multiple high-bandwidth channels (Bodurka et al., 2004), feeding in from multiple RF coils, has resulted, above all, in a dramatic increase in the image signal-to-noise ratio. Figure 9.3 illustrates the gains in sensitivity with multiple RF coils. Sensitivity is approximately proportional to the size of the RF coil used. In the past, some neuroimaging researchers chose to sacrifice brain coverage for sensitivity by using a single, large, "surface" RF coil for acquisition. Today, the use of multiple, small RF coils allows full brain coverage, at significantly higher sensitivity than one large RF coil. Recently, the Massachusetts Hospital Group constructed a brain-imaging device with 32 RF coils, leading to as much as a sixfold increase in signal to noise for an individual image, although, after taking into consideration unfilterable physiological noise, the gains are likely to be only about threefold. What the optimal number of coils might be with regard to increases in sensitivity remains uncertain.

Multichannel acquisition can also be conjoined with a novel image acquisition/reconstruction strategy that uses the spatially distinct sensitive region of each RF coil to help spatially encode the data—with only a small cost in signal to noise. This strategy is known as "SENSE [SENSitivity Encoding] imaging" (de Zwart et al., 2002). When coil placement is used to aid in spatial encoding, less time is needed to create an image of a given resolution. This advantage can be used in either of two ways: (1) the readout window width can be held the same, but the image resolution increased substantially; or (2) the image resolution can be held the same, but the width of the readout window decreased substantially. This reduction in readout window width allows a small increase in the number of EPI slices to be collected in a given repetition time (TR), therefore allowing a reduction in TR for a given number of slices, more slices for a given TR (allowing thinner slices perhaps), or an increase in brain coverage for a given TR (if a shorter TR had previously

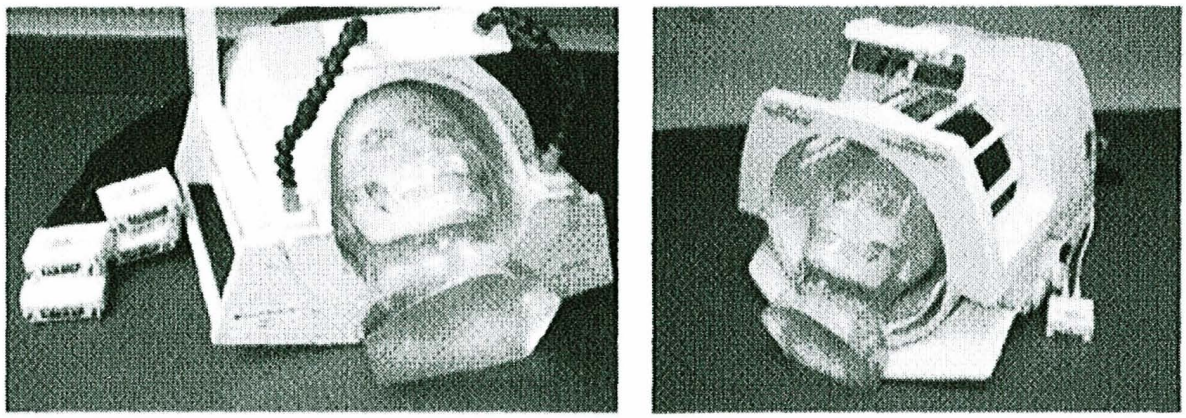

A B

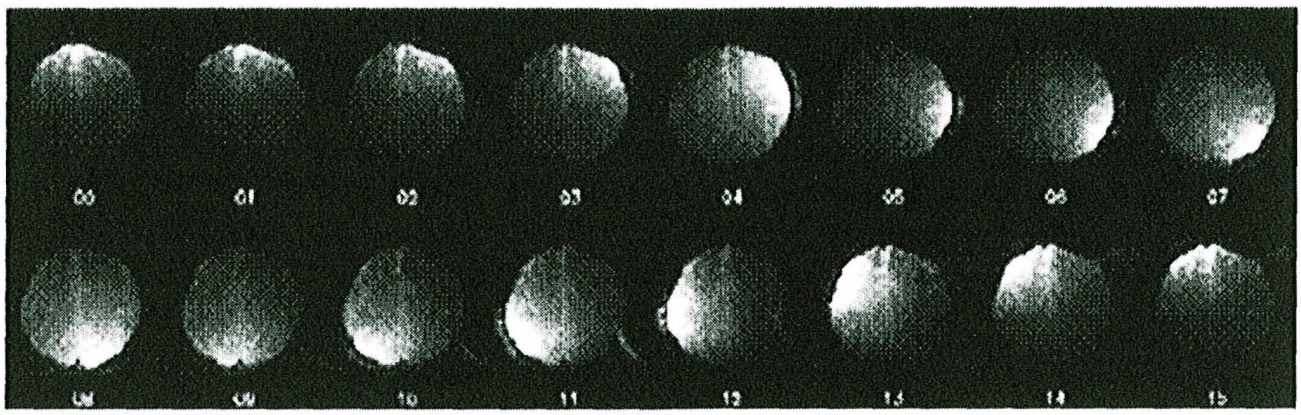

C

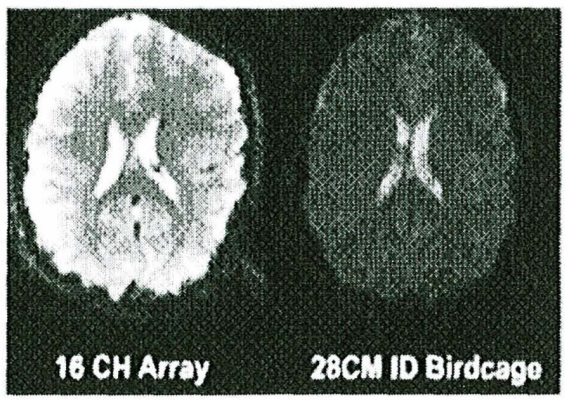

D

Figure 9.3
Comparison of image signal intensity of MR images created with single- and multichannel systems. (*A*) sixteen-channel coil system (NOVA Medical RF coil combined with NIH in-house parallel acquisition system. (*B*) Single-channel GE Medical Systems quadrature RF coil. (*C*) Display of distinct region of sensitivity for each of the 16 small RF coils within the NOVA Medical RF coil. (*D*) Image on the left was created by addition after reconstruction of the 16 individual images in panel C; image on the right was created from the GE Medical Systems quadrature RF coil. The two images being compared have been normalized such that the noise levels match. The signal intensity therefore gives a relative measure of signal to noise. (Figure provided courtesy of Jerzy Bodurka, Ph.D., Functional MRI Core Facility. The NOVA Medical 16 channel coil was designed by Jeff Duyn, Ph.D., Section on Advanced MRI, NINDS)

limited brain coverage). Incorporating this imaging strategy at field strengths above 3 T may allow robust single-shot echo planar imaging with a 1 mm^3 matrix size and a high-enough signal to noise for fMRI.

Free Behavior and Natural Stimuli Paradigms

A second innovation direction for fMRI lies in the domain of paradigm design. An ongoing challenge in fMRI is to have subjects perform tasks in a predictable and repeatable manner. This is not only impossible in many instances but limits the type of questions that can be addressed using fMRI. One common solution to this problem (described in the "Integration" section) is to keep track of the responses of subjects to specific tasks, then perform post hoc data averaging based on the responses. A potentially powerful extension of this idea is to collect a continuous measure of the subjects' free behavior. In this manner, a natural parametric variation in the response parameters can be used to guide data analysis. Any continuous measure will suffice. Subjects need simply to move a joystick or to track ball or to have their eye position or skin conductance monitored. They can be following an object, for example, or determining certainty, expectation, anxiety, or subjective perception of motion. The data collected can then be analyzed by calculating the moment-to-moment measurement and using it as a regressor in the analysis.

Related to paradigms that measure subjects' free behavior are those which measure their response to natural stimuli, as when viewing a movie, for example. Regressors can be calculated from various salient aspects of the movie presentation such as color, motion, volume, speech, or even the interaction of continuously measured eye position with these variables. A recently published study on movie viewing (Hasson et al., 2004) employed a highly novel processing technique, tailored to a specific paradigm. This technique was based on the understanding that, because the movie had many, unpredictable variables, it would be difficult to generate a set of reference functions for determining the similarly activated regions across subjects. What was done instead was to play precisely the same movie sequence at least twice for each subject and across all subjects. The assumption was that a distinct, repeatable temporal pattern would be manifest. Rather than attempting to choose an appropriate ideal reference function and comparing subsequent activation maps, Hasson and colleagues determined the correlation in the time series fMRI across subjects. Because this technique makes no assumption about what the data should look like—only that they show a repeatable change—it can be effectively applied for

the same subject across identical time series collections (see Levin and Uftring, 2001).

Real-Time fMRI Incorporating Feedback to the Subject

A technical challenge in fMRI is to perform basic analysis on data as they are being collected (Cox, Jesmanowicz, and Hyde, 1995). This approach is important for several reasons. A primary reason is to ensure data quality during the scan, an essential requirement if fMRI is to be incorporated into daily clinical practice. A secondary reason, and one just beginning to be explored, is to allow the person scanning or the subject being scanned to guide experimental process in real time. In this regard, some truly unique twists have recently been reported. Weiskopf et al. (2003) have determined that, when a measure of brain activation in specific regions activated by a cognitive (but not sensorimotor) task is fed back to subjects being imaged, they can learn, subjectively, to either increase or decrease the level of activation. This finding offers the fascinating possibility of humans interacting directly with and through computers through simple thought process regulation. Weiskopf's research group has trained subjects to play "pong" using mental control of a "paddle" in which the vertical location was simply proportional to the degree of activation in the controllable brain regions being activated. With two scanners collecting data simultaneously, subjects are able to successfully play "brain pong" using subjective control of their fMRI signal changes.

In a second study of this type of subjective control, DeCharms et al. (2004) instructed patients experiencing chronic pain to reduce the fMRI signal intensity in regions that had been associated with pain perception in a previous experiment. As in the "brain pong" experiment, the subjects were provided with feedback regarding the level of fMRI signal in these regions and were instructed to use whatever strategy they could come up with to decrease the signal. Not only did the experiment result in a subjective decrease in pain perception for most subjects, but this effect also appeared to last months after the experiment was carried out.

Direct Neuronal Current Imaging

A hope among brain imagers is for a technique that would allow direct mapping of brain activity with spatial resolution on the order of a cortical column *and* temporal resolution on the order of an action potential, or at

least of a postsynaptic potential. Recent work has established that, in ideal conditions, the minimal magnetic field change detectable with MRI is on the order of 1 ten billionth of a tesla (0.1 nT; Bodurka and Bandettini, 2002). Approximate calculations based on magnetoencephalography (MEG) measurements of 100 quadrillionths of a tesla (100 fT) at the surface of the skull estimate the magnetic field surrounding a dipole is also on the order of 0.1 nT. An increase in neuronal activity should be manifest as a highly localized, extremely transient magnitude decrease or phase shift in the MRI signal (Bandettini, Petridou, and Bodurka, forthcoming). Experimental groups attempting to detect this effect in humans have obtained mixed results, although some have claimed success (Konn et al., 2004; Xiang et al., 2003). Even if detecting the effect proves feasible, however, the utility of doing so will likely be limited, at least initially, by the extremely small size of the effect and the relatively small range of experiments possible using it due to the necessity for specific time-locked averaging. Nevertheless, because research efforts toward this goal have only begun, it is difficult to predict the ultimate success of this novel contrast approach.

Limitations

How accurately functional magnetic resonance imaging can assess brain activation is fundamentally limited by two major factors: (1) the method by which images are collected; and (2) the relationship between neuronal activity and hemodynamic changes.

Temporal Resolution

Echo planar images typically have an acquisition time of 30 msec. Assuming an echo time of 40 msec (the center of the readout window), data acquisition typically ends after 55 msec. About 15 msec is usually required to apply fat saturation at the beginning of the sequence and to apply gradients at the end to eliminate residual magnetization. Allowing for about 15 images to be collected in a second, the total time per plane for single-shot EPI time series collection is about 65 msec. For volume collection, which typically consists of 30 slices, a repetition time of 2 seconds is therefore required. It is also possible to collect one image (as opposed to multiple images) in a volume at a rate of 15 images per second over time.

As described, the hemodynamic response behaves like a low-pass filter for neuronal activity. At on/off frequencies of 6 sec on/6 sec off (0.08 Hz), BOLD responses begin to be attenuated relative to longer on/off times. At

on/off frequencies of 2 sec on/2 sec off (0.25 Hz), the BOLD response is almost completely attenuated. Even though BOLD attenuates these rapid on/off responses, activity of extremely brief duration can be observed. Activity durations as brief as 16 msec have been shown to cause robust BOLD signal changes, indicating that there is no apparent limit to the briefness of detectible activation. It is also heartening that, when repeated experiments are performed, the hemodynamic response in each voxel only shows a variability on the order of 100 msec.

Functional brain imagers wish not only to spatially resolve activated regions but also to determine the precise timing of activation in these regions relative both to the stimulus or input and to each other. The temporal resolution required for this type of assessment is on the order of at least tens of milliseconds. But, with BOLD contrast, the latency of the hemodynamic response has a range of 4 seconds due primarily to uncharacterized spatial variations in the underlying hemodynamics or neurovascular coupling from voxel to voxel, even within the same region of activity. If a voxel captures mostly larger venous vessels, the response is typically more delayed than if the voxel captures mostly capillaries, although the precise reasons for latency variations are as yet undetermined.

Of the methods proposed to solve the latency problem, the most direct (whose accuracy also remains undetermined, however) is to try to identify larger vessels by thresholding based on percent signal change or temporal fluctuation characteristics. Another solution is to use pulse sequences sensitive only to capillary effects. Arterial spin labeling techniques are more sensitive to capillaries, but the practical limitations of lower functional contrast to noise and longer interimage waiting time (due to the additionally required TI of about 1.5 sec) make this unworkable for most studies. Spin-echo sequences performed at very high field strengths or with velocity-nulling gradients (both of which eliminate intravascular large vessel effects) are also sensitive to capillary effects. On the other hand, since the reduction in functional contrast to noise is about a factor of 2 with spin-echo, and an additional factor of 3 with velocity-nulling gradients to remove intravascular signal, the contrast is likely too low to be useful.

An alternate strategy is to focus on localized *changes* in latency and width associated with task timing changes. As mentioned, within a voxel, the hemodynamic response varies on the order of 100 msec allowing significantly more accurate assessment when activation timing varies within a region. When neuroimagers use a task modulation that causes a difference in reaction time, and one region of the brain shows an increased width and another shows an increased delay, then it follows that the region showing

the width change is spending additional time to process information and the region showing the increased delay is downstream from the region showing the width change, having to wait until processing is complete in that node in order to receive any information. Although oversimplified, this scenario shows how temporal information may be extracted in fMRI. The key is task timing modulation and observation of hemodynamic changes, voxel by voxel.

Figure 9.4 (adapted from Bellgowan, Saad, and Bandettini, 2003) illustrates the point made above. Subjects performed a word recognition task in which the stimuli included both words and nonwords presented at varying rotation angles. Bellgowan, Saad, and Bandettini observed that subjects took longer to recognize nonwords than words, and longer to identify a word when it was rotated. The hypothesis is that the region performing word rotation and the region performing word recognition are likely to be spatially distinct. Figure 9.4 shows average time courses from the left anterior prefrontal cortex—typically associated with word generation. It appears that the hemodynamic response during word processing is about 500 msec wider than that during nonword processing, which suggests that activity in this region is of longer duration during the nonword recognition process.

Spatial Resolution

The upper in-plane resolution of standard single-shot echo planar imaging is about $2\,mm^2$. The use of multishot EPI (at a cost in time and stability) or of strategies incorporating multiple radiofrequency coils to aid in spatial encoding of data can achieve functional image resolutions of about $1\,mm^3$.

As with temporal resolution limits, spatial resolution limits are chiefly determined by the spatial spread of oxygenation and perfusion changes that accompany focal brain activation, not by limits in acquisition. Although the "hemodynamic point-spread function" has been empirically determined to be on the order of $3\,mm^3$ (Engel, Glover, and Wandell, 1997), the effects of draining veins have been observed to be as distal as 1 cm from focal regions of activation identified using perfusion contrast.

The pulse-sequence solutions for dealing with the variations in hemodynamics have proved as effective as those for dealing with temporal resolution limits. Moreover, working with hypercapnia comparisons, Bandettini and Wong (1997) and Cohen et al. (2004) have proposed spatial calibration methods. Using BOLD fMRI methods based on cerebral perfusion and blood volume, other brain imagers have delineated ocular dominance

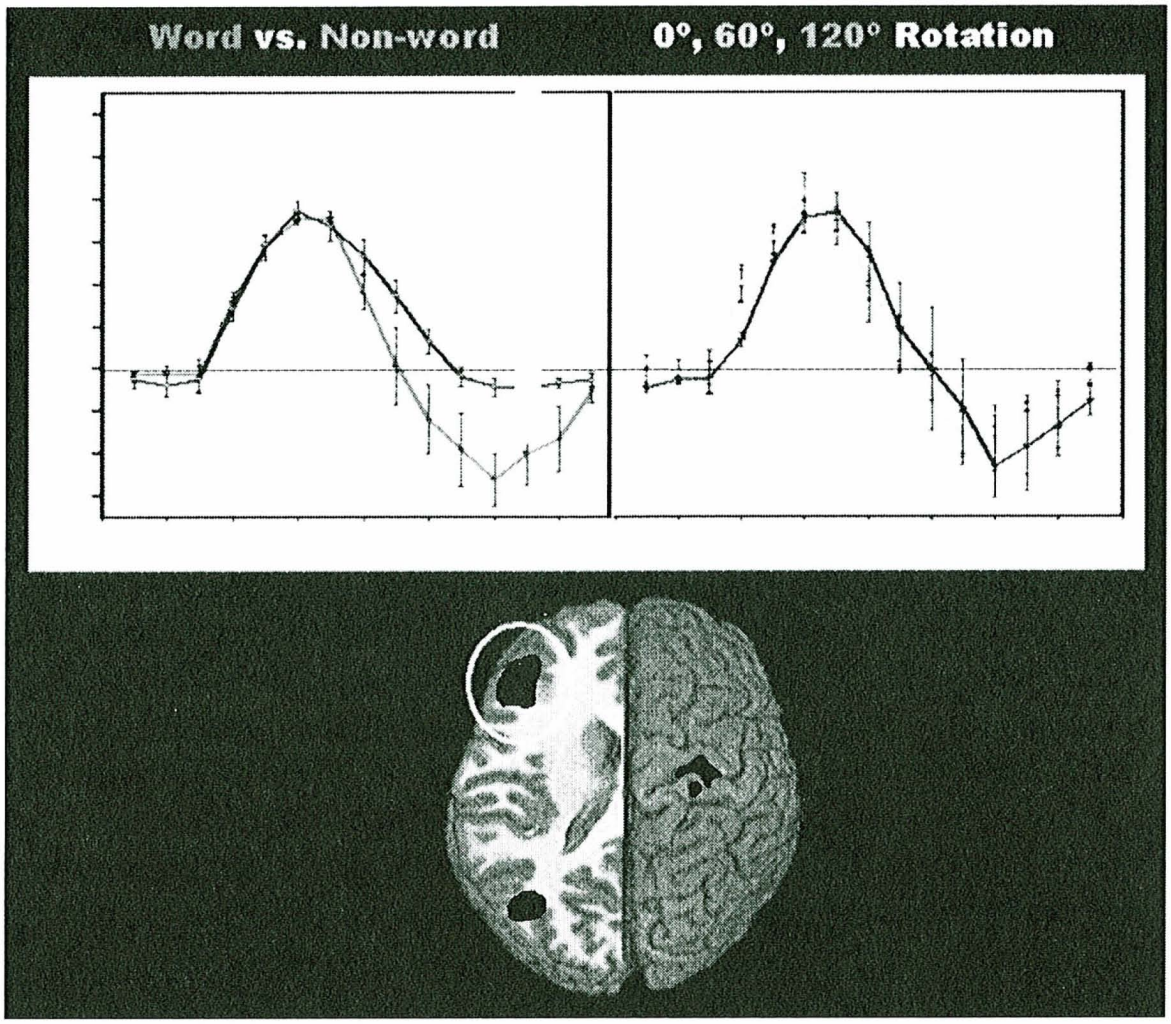

Figure 9.4
Averaged time courses from the left anterior prefrontal cortex during a word recognition task in which the words were presented at varying rotation angles. When word and nonword processing are compared, the width of the hemodynamic response is wider by about 500 msec, suggesting that there is longer duration of activity in this region during the nonword recognition process. When angles of rotation are compared, the onset of activation in this region appears delayed as a function of angle of rotation, suggesting that this region is downstream from the region associated with word rotation. (Adapted from Bellgowan, Saad, and Bandettini, 2003)

columns (1 mm^3; Cheng, Waggoner, and Tanaka, 2001; Goodyear and Menon, 2001) and cortical layers (< 0.5 mm^3; Logothetis et al., 2002), although, with BOLD contrast (thought to have the lowest resolution), columnar and layer specificity was achieved only by subtracting activation from tasks activating interspersed yet distinct regions (i.e., columns or layers). An ongoing issue with regard to the upper resolution of fMRI is whether or not *fine* delineation necessarily translates to *accurate* delineation—meaning that detailed activation maps may not precisely register underlying function.

Interpretation

Considerable effort has been directed toward understanding the precise relationship between fMRI signal changes and neuronal activity. Strategies for overcoming limits to interpretation of the data gathered have included

- animal models and the simultaneous use of other measures of neuronal activity such as multiunit electrodes or more precise measures of hemodynamic changes, such as optical imaging;
- parametric modulation of magnitude or timing of activation in humans with corresponding measurement of fMRI signal changes;
- simultaneous measures of neuronal activity (implanted electrode or EEG) and fMRI signal changes;
- nonsimultaneous MEG or EEG measures of neuronal activity and fMRI signal changes; and
- modeling the hemodynamic response and comparing model outputs to precise activation magnitude, timing, or pharmacological manipulations of brain tissue.

In summary, even though fMRI is limited to a lesser degree by scanner technology and to a greater degree by the unknowns regarding the spatial, temporal, and magnitude relationships between neuronal activity and hemodynamic signal changes, steady progress is being made in overcoming these limitations. A primary avenue by which the limitations of functional magnetic resonance imaging can be overcome is integration with other brain activation assessment techniques.

Integration

Functional MRI data collection and even the experimental process itself can be greatly enhanced in precision, depth, impact, and certainty if researchers

effectively incorporate other brain activation assessment techniques ranging from behavioral to other imaging approaches (Dale and Halgren, 2001).

Techniques that can be simultaneously carried out during time series collection of fMRI data include

- behavioral measures such as performance, reaction time, skin conductance, and eye position;
- electroencephalography (EEG);
- embedded electrodes or multielectrode arrays;
- near-infrared spectroscopy (NIRS) or optical imaging;
- transcranial magnetic stimulation (TMS); and
- physiological measures such as respiration, heart rate, end tidal carbon dioxide, and skin conductance.

Although simultaneity is desirable, complementary experimental measures can be effectively integrated without it. It is only necessary that they be precisely repeatable. Techniques in which the data are collected before or after fMRI experimentation include not only those listed above but also

- positron-emission tomography (PET) and
- magnetoencephalography (MEG).

Although this section describes the methodology and utility of only several of many ways that fMRI experimentation, analysis, and results can be integrated with other modalities, readers are encouraged to consult the relevant chapters in this volume for a more detailed discussion of the specific techniques.

Behavioral Measures

Depending on the hypothesis posed, substantial inferences about brain activity can be made from simple measures of response accuracy and response time, although, since the beginnings of functional MRI experimentation, behavioral response data have also been collected to ensure that the subjects are actually engaged in the experimental tasks assigned them. Subject interface devices such as button boxes or joysticks have been and typically still are used. With the onset of rapid event-related fMRI, however, the ability to selectively average data based on behavioral responses from moment to moment has further increased the range of experiments possible with fMRI.

Two studies, both of processes associated with memory but using different methodologies, serve to illustrate effective integration of behavioral measures with fMRI. In Wagner et al., 1998, subjects were presented with lists of words during the time series collection of fMRI data, which were selectively binned, based on whether the subjects recalled the words after the scanning process. Results revealed that the ability to later remember a verbal experience was predicted by the magnitude of activation in left prefrontal and temporal cortices during that experience.

In Pessoa et al., 2002, fMRI was used to investigate how moment-to-moment neural activity contributed to success or failure on individual trials of a visual working memory task. Different nodes of the network involved with working memory were found to be activated to a greater extent for correct than for incorrect trials during stimulus encoding, memory maintenance during delays, and at test. A logistic regression analysis revealed that the fMRI signal amplitude during the delay interval in a network of frontoparietal regions predicted successful performance trial by trial. Differential activity during the delay periods when working memory was active occurred even on trials when BOLD activity during encoding was strong, demonstrating that such differential activity was not a simple consequence of effective versus ineffective encoding. Study results further demonstrated that accurate memory depends on strong, sustained signals that span the delay interval of working memory tasks. These results could not have been achieved without precise measures of behavior either after the scanning process (testing for long-term memory) or during the scanning process (testing for working memory).

In general, some of the most insightful fMRI results have resulted from tight integration of moment-to-moment behavioral measures with time series collection, which allows researchers to selectively bin relevant fMRI data. Other behavioral measures have included reaction time, eye position, measures of decision processes, and continuous measures of performance or mental state such as those obtained by the use of a joystick or trackball.

Electroencephalography and Magnetoencephalography

The signals produced by EEG and MEG are more direct measures of neuronal activity than those produced with functional MRI, reflecting the electric potential (EEG) and the magnetic field (MEG) resulting from synaptic currents in neuronal dendrites. On the other hand, because of the inherently ill posed "inverse problem" regarding localization of the dipole sources contributing to the electrical potentials and magnetic fields on the

surface of the skull, the resolution or, rather, the certainty of localization for both EEG and MEG is generally quite low. Integration of these two techniques and fMRI, however, allows neuroimagers to map brain activity at the higher spatial resolution of fMRI (effectively constraining the "inverse problem"), but also at the higher temporal resolution afforded by MEG and EEG. This will be discussed in greater detail when describing integration with MEG below (see also Singh, chapter 12, this volume). Also, simultaneous use of EEG with fMRI can enhance the ability of neuroimagers to map spontaneous and transient processes only detectible by EEG but mappable using hemodynamic responses that occur 3 to 10 seconds after a signature EEG response.

The complementary use of EEG and fMRI is a burgeoning field in itself: since 1997, over 200 papers have been published on this topic alone. A primary use of simultaneous EEG and fMRI data collection is for the accurate measurement of hemodynamic changes associated with spontaneously occurring and transient events measurable with EEG (see Lemieux, 2003). Another use of these simultaneous measures has been to compare the time-locked, averaged, evoked response characteristics with the hemodynamic response characteristics in order to better understand the neuronal correlates of fMRI. These experiments do not require simultaneous EEG and fMRI but the results derived with simultaneous acquisition are likely to be more accurate since no experiment is replicated perfectly inside and outside of the scanner.

A promising clinical application of simultaneous EEG and fMRI is the more accurate localization of epileptic foci. In specific clinical populations, these foci exhibit spontaneous, irregular EEG activity. The use of simultaneous EEG and fMRI allows neuroimagers to selectively average functional images based on when this signature activity occurs.

In another unique application, simultaneous EEG and fMRI can be used to determine the neuronal correlates of spontaneously changing brain activity associated with specific EEG frequencies. After simultaneously measuring EEG and fMRI, neuroimagers create the power spectrum of the EEG traces for each repetition time (TR) period. They then convolve the amplitude of the power spectrum at a specific frequency range (for example, alpha frequencies: 8–12 Hz, and beta frequencies: 17–23 Hz) at each TR with a hemodynamic response function, used as a regressor in fMRI time series analysis. Taking this approach, Goldman et al. (2001) and Laufs et al. (2003a, 2003b) have been able to accurately map regions that exhibit changes in the hemodynamic response that correlate with spontaneous changes in oscillatory activity.

Simultaneous use of EEG and fMRI data is challenging because the concomitant collection of echo planar imaging data creates a substantial artifact in the EEG trace whenever magnetic field gradients are applied. Several strategies have succeeded in filtering out this artifact however: simply discarding EEG points that occur during image collection; using hardware-based filters or more sophisticated postprocessing techniques; and using what is known as "spike-triggered fMRI scanning", in which unique EEG activity (i.e., spiking) triggers the scanner to collect images.

Efforts to integrate MEG and fMRI (see Dale and Halgren, 2001) have begun to increase as MEG systems become more available, and as the interpretive limits of using fMRI alone become more apparent. Because MEG and fMRI data cannot be collected simultaneously, however, the effectiveness of the integration depends on precise experimental replicability.

Another highly challenging but potentially promising procedure integrating MEG or EEG and fMRI uses fMRI activation maps to help determine dipole locations. The potential information gained by this procedure is significant: when dipole sources for a given cognitive process are precisely determined, the inverse problem can be replaced by a much more readily solvable forward problem. Starting with the dipole locations, the relative dynamics of measured fields at the surface of the skull can then be used to infer the dipole source timings with millisecond accuracy (Ahlfors et al., 1999).

While the promise of precisely determining dipole sources with fMRI data is exciting, many problems remain. First, if there exist mismatches between fMRI activation foci and the true dipole sources, substantial misestimates in timing will result. In this sense, the timing estimation is quite "brittle" in that any errors in dipole estimation render the results almost uninterpretable. Growing evidence exists that there are, in fact, substantial differences between fMRI activation maps and MEG visible dipole sources. With MEG, opposing dipoles may cancel each other, rendering their effects invisible to fMRI. With fMRI, false positives are ubiquitous in individual data, and, likewise, it is not certain whether all MEG-sensitive effects contribute to hemodynamic changes. Also, cognitive tasks typically involve highly distributed networks within and across distributed regions that generally defy simplification to a set of dipoles. Currently, effort is being made to estimate the certainty of the dipole sources, and thus to increase the flexibility and robustness of this approach.

A central issue in the integration of EEG or MEG and fMRI data and, more generally, in the interpretation of fMRI signal changes is that of clarifying the relationship between neuronal activity and fMRI signal changes.

To this end, substantial effort has been applied using other modalities to better understand fMRI contrast. Fruitful studies representing only a small fraction of this effort include those using MEG (Singh et al., 2002), EEG (Horovitz, Skudlarski, and Gore, 2002), optical imaging (Grinvald, Slovin, and Vanzetta, 2000; Villringer, 1997; Cannestra et al., 2001; Boas, Dale, and Franceschini, 2004), electrophysiological recording in humans (Huettel et al., 2004) and animal models (Logothetis et al., 2001; Duong et al., 2000; Devor et al., 2003) and microscopic oxygen probes in animal models (Thompson, Peterson, and Freeman, 2003, 2004).

Transcranial Magnetic Stimulation

In TMS, a highly localized, rapidly oscillating magnetic field is directed at specific circuits of the brain. This rapid oscillation induces neuronal activity, thereby disrupting normal function for what is thought to be a very brief period of time. The power of this technique is its ability to probe the necessity of specific nodes in a network as they relate to specific processes. Because a central problem in the interpretation of brain activation maps is that of determining causality, TMS is highly complementary to brain mapping techniques. Thus it is not apparent from such maps which nodes are activated as a result of actually performing the task and which are activated in order to perform the task. By allowing specific nodes of an activation network to be temporarily disabled, observation of behavior associated with the application of TMS can tease apart the causality of the network involved (Lomarev et al., 2000). The additional dimension of neuronal timing can also be explored by modulating the TMS application time relative to stimulus and response timing. Typically, the TMS timing is titrated to determine the interval that most effectively interferes with a specific behavioral process, thereby revealing neuronal communication rates.

Typically, with TMS and fMRI integration, a brain activation map is first produced and then used to guide TMS stimulation outside of the scanner. Some groups, however, by performing TMS *during* collection of fMRI time series data, have been able to probe the effects of TMS, in itself, on brain activation and thereby to assess functional connectivity against the assumption that if one node is activated, then the nodes it is functionally associated with will also be activated (Bohning et al., 2000a, 2000b). This application, one should note, is highly challenging and may be risky since the torque generated by interaction of the strong electrical currents of a TMS device (typically a figure-eight loop of wire) with the scanner mag-

netic field can be substantial, depending on the orientation (Bohning et al., 2003).

Because, relatively speaking, TMS devices are inexpensive, easy to operate, and noninvasive, and because the information this technique provides is highly complementary to the data provided by fMRI, TMS is growing rapidly in popularity.

Physiological Measures

A growing trend in fMRI data collection has been not only toward simultaneous recording of behavioral responses but also toward simultaneous collection of physiological measures such as heart and respiration waveforms, end tidal carbon dioxide, and skin conductance. The information gleaned from these measures ranges from assessment and reduction of artifactual influences on the BOLD response to assessment and use of measures of arousal and attention.

Respiration and cardiac pulsations are known to contribute to artifactual signal changes in fMRI, from changes in the magnetic field caused either by the chest cavity movement (respiration; Windischberger et al., 2002; Pfeuffer et al., 2002a) or by localized acceleration of blood, cerebral spinal fluid, and brain tissue (cardiac pulsations; Dagli, Ingeholm, and Haxby, 1999). By simply recording respiration with a chest bellows and cardiac pulsation with a pulse oximeter, neuroimagers can use these artifactual waveforms as "nuisance" regressors, thereby effectively increasing functional contrast to noise and reducing false positive results.

A challenge in removing cardiac effects is that the repetition time is typically too low to sample the cardiac waveform sufficiently. Methods have been proposed to work around this problem (Frank, Buxton, and Wong, 2001; Menon, 2002; Noll et al., 1998). For some fMRI studies, the movement artifacts caused by cardiac pulsations, particularly at the base of the brain, are prohibitive—particularly when attempting to image very small structures that may displace several voxels with each cardiac cycle. This problem has been effective solved by a novel method involving cardiac gating, which subsequently corrects T1-related fluctuations from irregular repetition time values (Guimaraes et al., 1998).

An ongoing study of spontaneous end tidal carbon dioxide fluctuations (Wise et al., 2004) has revealed useful information about the nature of BOLD time series fluctuations. Maps generated using spontaneous changes in end tidal carbon dioxide appear to delineate the spatial distribution of resting-state venous blood volume, indicating the potential for

BOLD signal changes at the voxel level. This study also gives strong evidence that simple changes in breathing rate and depth during an experiment can influence BOLD signal changes. The above three measures may prove to have a complementary impact on the expanding research into resting-state fluctuations to elucidate functionally correlated resting networks (see Lowe, Mock, and Sorenson, 1998; Gusnard et al., 2001; Biswal et al., 1995).

A fourth physiological measure, skin conductance, is a sensitive indicator of states such as arousal, attention, and anxiety. Skin conductance data have also been successfully collected at the same time as fMRI time series data (Critchley et al., 2000; Patterson, Ungerleider, and Bandettini, 2002, Williams et al., 2000; Shastri et al., 2001).This has been done to serve two distinct reseach ends: (1) to ensure that subjects are exhibiting the appropriate response to specific stimuli; and (2) to demonstrate the neuronal correlates of skin conductance in specific mental states or during resting state. Figure 9.5 shows time course plots from an experiment that involved conditioning subjects to expect a shock when they heard a tone presented during the conditioned-stimulus (CS) period (Knight, Nguyen, and Bandettini, 2005).

To serve the second research end, simultaneous measures of skin conductance are used is in much the same way as simultaneous EEG measures, only in this case, SCR time course data are correlated with fMRI time series data. Thus Patterson, Ungerleider, and Bandettini (2002) measured spontaneous skin conductance changes continuously during specific tasks and resting state. Using the spontaneous skin conductance measurement as a regressor, they identified a specific set of regions that showed activity that was correlated with skin conductance changes independent of the task being performed.

Conclusion

This chapter represents only a grainy snapshot of a rapidly changing scene. Its aim has been to give at least some sense of the history, development, limits, and more innovative ideas of functional MRI, and of the general excitement surrounding this rapidly advancing technique. Integration of fMRI with other techniques is steadily contributing to our understanding of how the human brain is organized, how it changes from moment to moment and year to year, and how it varies across clinically relevant populations. Although it is still too early to tell what the ultimate impact of fMRI will be have on the fields of neuroscience and medicine, one thing is

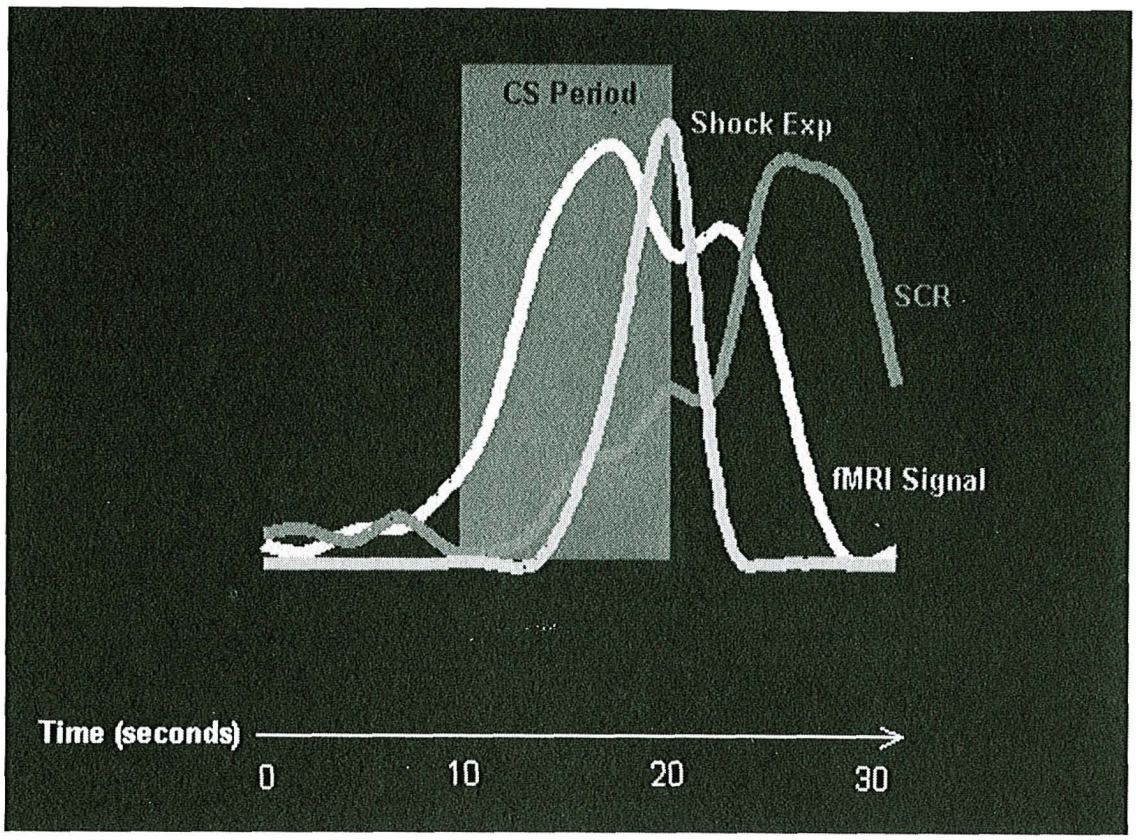

Figure 9.5
Time course plots from an experiment (Knight, Nguyen, and Bandettini, forthcoming) involved conditioning subjects to expect a shock when they heard a tone during the conditioned stimulus (CS) period. Subjects controlled a dial according to subjective expectation level; their skin conductance response (SCR) was also continuously measured. (Figure provided courtesy of David Knight, Ph.D., Section on Functional Imaging Methods, NIMH)

already clear: functional magnetic resonance imaging is a maturing technique with extraordinary potential.

Acknowledgments

This work was supported by the National Institute of Mental Health (NIMH), Division of Intramural Research Programs. My thanks to Ziad Saad, Scientific and Statistical Core Facility; David Knight, Section on Functional Imaging Methods; and Jerzy Bodurka, Functional MRI Core Facility, all of the NIMH, for their contributions of figures to this chapter.

References

Ahlfors, S. P., Simpson, G. V., Dale, A. M., Belliveau, J. W., Liu, A. K., Korvenoja, A., Virtanen, J., Huotilainen, M., Tootell, R. B. H., Aronen, H. J., and Ilmoniemi,

R. J. (1999). Spatiotemporal activity of a cortical network for processing visual motion revealed by MEG and fMRI. *Journal of Neurophysiology*, *82*, 2545–2555.

An, H. Y., Lin, W. L., Celik, A., and Lee, Y. Z. (2001). Quantitative measurements of cerebral metabolic rate of oxygen using MRI: A volunteer study. *NMR in Biomedicine*, *14*, 441–447.

Bandettini, P. A., Jesmanowicz, A., Wong, E. C., and Hyde, J. S. (1993). Processing strategies for time-course data sets in functional MRI of the human brain. *Magnetic Resonance Medicine*, *30*, 161–173.

Bandettini, P. A., Petridou, N., and Bodurka, J. (2006). Direct detection of neuronal activity with MRI: Fantasy, possibility, or reality? *Applied Magnetic Resonance*, *29*, 65–85.

Bandettini, P. A., and Wong, E. C. (1997). A hypercapnia-based normalization method for improved spatial localization of human brain activation with fMRI. *NMR in Biomedicine*, *10*, 197–203.

Bandettini, P. A., Wong, E. C., Hinks, R. S., Tikofsky, R. S., and Hyde, J. S. (1992). Time course EPI of human brain functioning during task activation. *Magnetic Resonance in Medicine*, *25*, 390–397.

Beckmann, C. F., and Smith, S. A. (2004). Probabilistic independent component analysis for functional magnetic resonance imaging. *IEEE Transactions on Medical Imaging*, *23*, 137–152.

Bellgowan, P. S. F., Saad, Z. S. and Bandettini, P. A. (2003). Understanding neural system dynamics through task modulation and management. *Proceedings of the National Academy of Sciences, USA*, *100*, 1415–1419.

Belliveau, J. W., Kennedy, D. N., McKinstry, R. C., Buchbinder, B. R., Weisskoff, R. M., Cohen, M. S., Vevea, J. M., Brady, T. J., and Rosen, B. R. (1991). Functional mapping of the human visual cortex by magnetic resonance imaging. *Science*, *254*, 716–719.

Binder, J. R., Frost, J. A., Hammeke, T. A., Bellgowan, P. S. F., Rao, S. M., and Cox, R. W. (1999). Conceptual processing during the conscious resting state: A functional MRI study. *Journal of Cognitive Neuroscience*, *11*, 80–93.

Binder, J. R. Frost, J. A., Hammeke, T. A., Cox, R. W., Rao, S. M., and Prieto, T. (1997). Human brain language areas identified by functional magnetic resonance imaging. *Journal of Neuroscience*, *17*, 353–362.

Binder, J. R., Rao, S. M., Hammeke, T. A., Frost, J. A., Bandettini, P. A., and Hyde, J. S. (1994). Effects of stimulus rate on signal response during functional magnetic resonance imaging of auditory cortex. *Cognitive Brain Research*, *2*, 31–38.

Biswal, B., Yetkin, F. Z., Haughton, V. M., and Hyde, J. S. (1995). Functional connectivity in the motor cortex of resting human brain using echo-planar MIR. *Magnetic Resonance in Medicine*, *34*, 537–541.

Blamire, A. M., Ogawa, S., Ugurbil, K., Rothman, D., McCarthy, G., Ellermann, J. M., Hyder, F., Rattner, Z., and Shulman, R. G. (1992). Dynamic mapping of the

human visual cortex by high-speed magnetic resonance imaging. *Proceedings of the National Academy of Sciences, USA*, *89*, 11069–11073.

Boas, D. A., Dale, A. M., and Franceschini, M. A. (2004). Diffuse optical imaging of brain activation: Approaches to optimizing sensitivity, resolution and accuracy. *NeuroImage*, *23*, S275–S288.

Bodurka, J., and Bandettini, P. A. (2002). Toward direct mapping of neuronal activity: MRI detection of ultraweak, transient magnetic field changes. *Magnetic Resonance in Medicine*, *47*, 1052–1058.

Bodurka, J., Ledden, P. J., van Gelderen, P., Chu, R. X., de Zwart, J. A., Morris, D., and Duyn, J. H. (2004). Scalable multichannel MRI data acquisition system. *Magnetic Resonance in Medicine*, *51*, 165–171.

Bohning, D. E., Denslow, S., Bohning, P. A., Walker, J. A., and George, M. S. (2003). A TMS coil positioning/holding system for MR image-guided TMS interleaved with fMRI. *Clinical Neurophysiology*, *114*, 2210–2219.

Bohning, D. E., Shastri, A., McGavin, L., McConnell, K. A., Nahas, Z., Lorberbaum, J. P., Roberts, D. R., and George, M. S. (2000a). Motor cortex brain activity induced by 1 Hz transcranial magnetic stimulation is similar in location and level to that for volitional movement. *Investigative Radiology*, *35*, 676–683.

Bohning, D. E., Shastri, A., Wassermann, E. M., Ziemann, U., Lorberbaum, J. P., Nahas, Z., Lomarev, M. P., and George, M. S. (2000b). BOLD-fMRI response to single-pulse transcranial magnetic stimulation (TMS). *Journal of Magnetic Resonance Imaging*, *11*, 569–574.

Botvinick, M., Nystrom, L. E., Fissell, K., Carter, C. S., and Cohen, J. D. (1999). Conflict monitoring versus selection-for-action in anterior cingulated cortex. *Nature*, *402*, 179–181.

Boynton, G. M., Engel, S. A., Glover, G. H., and Heeger, D. J. (1996). Linear systems analysis of functional magnetic resonance imaging in human V1. *Journal of Neuroscience*, *16*, 4207–4221.

Braver, T. S., Cohen, J. D., Nystrom, L. E., Jonides, J., Smith, E. E., and Noll, D. C. (1997). A parametric study of prefrontal cortex involvement in human working memory. *NeuroImage*, *5*, 49–62.

Breiter, H. C., Etcoff, N. L., Whalen, P. J., Kennedy, W. A., Rauch, S. L., Buckner, R. L., Strauss, M. M., Hyman, S. E., and Rosen, B. R. (1996). Response and habituation of the human amygdala during visual processing of facial expression. *Neuron*, *17*, 875–887.

Buchel, C., and Friston, K. J. (1998). Dynamic changes in effective connectivity characterized by variable parameter regression and kalman filtering. *Human Brain Mapping*, 6, 403–408.

Buckner, R. L., Bandettini, P. A., O'Craven, K. M., Savoy, R. L., Petersen, S. E., Raichle, M. E., and Rosen, B. R. (1996). Detection of cortical activation

during averaged single trials of a cognitive task using functional magnetic imaging. *Proceedings of the National Academy of Sciences, USA, 93*, 14878–14883.

Buckner, R. L., Petersen, S. E., Ojemann, J. G., Miezin, F. M., Squire, L. R., and Raichle, M. E. (1995). Functional anatomical studies of explicit and implicit memory retrieval tasks. *Journal of Neuroscience, 15*, 12–29.

Bush, G., Luu, P., and Posner, M. I. (2000). Cognitive and emotional influences in anterior cingulate cortex. *Trends in Cognitive Science, 4*, 215–222.

Buxton, R. B., and Frank, L. R. (1997). A model for the coupling between cerebral blood flow and oxygen metabolism during neural stimulation. *Journal of Cerebral Blood Flow and Metabolism, 17*, 64–72.

Buxton, R. B., Uludag, K., Dubowitz, D. J., and Liu, T. T. (2004). Modeling the hemodynamic response to brain activation. *NeuroImage, 23*, S220–S233.

Cabeza, R., and Nyberg, L. (2000). Imaging cognition II: An empirical review of 275 PET and fMRI studies. *Journal of Cognitive Neuroscience, 12*, 1–47.

Cannestra, A. F., Pouratian, N., Bookheimer, S. Y., Martin, N. A., Beckerand, D. P., and Toga, A. W. (2001). Temporal spatial differences observed by functional MRI and human intraoperative optical imaging. *Cerebral Cortex, 11*, 773–782.

Carter, C. S., Braver, T. S., Barch, D. M., Botvinick, M. M., Noll, D., and Cohen, J. D. (1998). Anterior cingulate cortex, error detection, and the online monitoring of performance. *Science, 280*, 747–749.

Cheng, K., Waggoner, R. A., and Tanaka, K. (2001). Human ocular dominance columns as revealed by high-field functional magnetic resonance imaging. *Neuron, 32*, 359–374.

Cohen, E. R., Rostrup, E., Sidaros, K., Lund, T. E., Paulson, O. B., Ugurbil, K., and Kim, S. G. (2004). Hypercapnic normalization of BOLD fMRI: Comparison across field strengths and pulse sequences. *NeuroImage, 23*, 613–624.

Cohen, J. D., Perlstein, W. M., Braver, T. S., Nystrom, L. E., Noll, D. C., Jonides, J., and Smith, E. E. (1997). Temporal dynamics of brain activation during a working memory task. *Nature, 386*, 604–608.

Corbetta, M., Akbudak, E., Conturo, T. E., Snyder, A. Z., Ollinger, J. M., Drury, H. A., Linenweber, M. R., Petersen, S. E., Raichle, M. E., Van Essen, D. C., and Shulman, G. L. (1998). A common network of functional areas for attention and eye movements. *Neuron, 21*, 761–773.

Corbetta, M., and Shulman, G. L. (2002). Control of goal-directed and stimulus-driven attention in the brain. *Nature Reviews Neuroscience, 3*, 201–215.

Corbetta, M., Kincade, J. M., Ollinger, J. M., McAvoy, M. P., and Shulman, G. L. (2000). Voluntary orienting is dissociated from target detection in human posterior parietal cortex. *Nature Neuroscience, 3*, 292–297.

Courtney, S. M., Petit, L., Maisog, J. M., Ungerleider, L. G., and Haxby, J. V. (1998). An area specialized for spatial working memory in human frontal cortex. *Science, 279*, 1347–1351.

Courtney, S. M., Ungerleider, L. G., Keil, K., and Haxby, J. V. (1996). Object and spatial visual working memory activate separate neural systems in human cortex. *Cerebral Cortex*, *6*, 39–49.

Courtney, S. M., Ungerleider, B. G., Keil, K., and Haxby, J. V. (1997). Transient and sustained activity in a distributed neural system for human working memory. *Nature*, *386*, 608–611.

Cox, R. W. (1996). Software for analysis and visualization of functional magnetic resonance neuroimages. *Computers and Biomedical Research*, *29*, 162–173.

Cox, R. W., Jesmanowicz, A., and Hyde, J. S. (1995). Real-time functional magnetic resonance imaging. *Magnetic Resonance in Medicine*, *33*, 230–236.

Critchley, H. D., Elliott, R., Mathias, C. J., and Dolan, R. J. (2000). Neural activity relating to the generation and representation of galvanic skin conductance response: A functional magnetic resonance imaging study. *Journal of Neuroscience*, *20*, 3033–3040.

Dagli, M. S., Ingeholm, J. E., and Haxby, J. V. (1999). Localization of cardiac-induced signal change in fMRI. *NeuroImage*, *9*, 407–415.

Dale, A. M., and Buckner, R. L. (1997). Selective averaging of rapidly presented individual trials using fMRI. *Human Brain Mapping*, *5*, 329–340.

Dale, A. M., Fischl, B., and Sereno, M. I. (1999). Cortical surface-based analysis. 1. Segmentation and surface reconstruction. *NeuroImage*, *9*, 179–194.

Dale, A. M., and Halgren, E. (2001). Spatiotemporal mapping of brain activity by integration multiple imaging modalities. *Current Opinion in Neurobiology*, *11*, 202–208.

Davis, T. L., Kwong, K. K., Weisskoff, R. M., and Rosen, B. R. (1998). Calibrated functional MRI: Mapping the dynamics of oxidative metabolism. *Proceedings of the National Academy of Sciences, USA*, *95*, 1834–1839.

DeCharms, R. C., Christoff, K., Glover, G. H., Pauly, J. M., Whitfield, S., and Gabrieli, J. D. E. (2004). Learned regulation of spatially localized brain activation using real-time fMRI. *NeuroImage*, *21*, 436–443.

Demb, J. B., Desmond, J. E., Wagner, A. D., Vaidya, C. J., Glover, G. H., and Gabrieli, J. D. (1995). Semantic encoding and retrieval in the left inferior prefrontal cortex–A functional MRI study of task difficulty and process specificity. *Journal of Neuroscience*, *15*, 5870–5878.

D'Esposito, M., Detre, J. A., Alsop, D. C., Shin, R. K., Atlas, S., and Grossman, M. (1995). The neural basis of the central executive system of working memory. *Nature*, *378*, 279–281.

Devor, A., Dunn, A. K., Andermann, M. L., Ulbert, I., Boas, D. A., and Dale, A. M. (2003). Coupling of total hemoglobin concentration, oxygenation, and neural activity in rat somatosensory cortex. *Neuron*, *39*, 353–359.

DeYoe, E. A., Bandettini, P., Neitz, J., Miller, D., and Winans, P. (1994). Functional magnetic resonance imaging (fMRI) of the human brain. *Journal of Neuroscience Methods*, *54*, 171–187.

de Zwart, J. A., van Gelderen, P., Kellman, P., and Duyn, J. H. (2002). Application of sensitivity-encoded echo-planar imaging for blood oxygen level–dependent functional brain imaging. *Magnetic Resonance in Medicine*, *48*, 1011–1020.

Duong, T. Q., Kim, D. S., Ugurbil, K., and Kim, S. G. (2000). Spatio-temporal dynamics of the BOLD fMRI signals in cat visual cortex: Toward mapping columnar structures using early negative response. *Magnetic Resonance in Medicine*, *44*, 231–242.

Edmister, W. B., Talavage, T. M., Ledden, P. J., and Weisskoff, R. M. (1999). Improved auditory cortex imaging using clustered volume acquisitions. *Human Brain Mapping*, *7*, 89–97.

Egan, M. F., Goldberg T. E., Kolachana, B. S., Callicott, J. H., Mazzanti, C. M., Straub, R. E., Goldman, D., and Weinberger, D. R. (2001). Effect of COMT Val(108/158) Met genotype on frontal lobe function and risk for schizophrenia. *Proceedings of the National Academy of Sciences*, *98*, 6917–6922.

Egan, M. F., Kojima, M., Callicott, J. H., Goldberg, T. E., Kolachana, B. S., Bertolino, A., Zaitsev, E., Gold, B., Goldman, D., Dean, M., Lu, B., and Weinberger, D. R. (2003). The BDNF val66met polymorphism affects activity-dependent secretion of BDNF and human memory and hippocampal function. *Cell*, *112*, 257–269.

Engel, S. A., Glover, G. H., and Wandell, B. A. (1997). Retinotopic organization in human visual cortex and the spatial precision of functional MRI. *Cerebral Cortex*, *7*, 181–192.

Engel, S. A., Rumelhart, D. E., Wandell, B. A., Lee, A. T., Glover, G. H., Chichilnisky, E. J., and Shadlen, M. N. (1994). fMRI of human visual cortex. *Nature*, *369*, 525–525.

Fischl, B., Sereno, M. I., Tootell, R. B. H., and Dale, A. M. (1999). High-resolution inter-subject averaging and a coordinate system for the cortical surface. *Human Brain Mapping*, *8*, 272–284.

Fletcher, P. C., and Henson, R. N. A. (2001). Frontal lobes and human memory—Insights from functional neuroimaging. *Brain*, *124*, 849–881.

Forman, S. D., Cohen, J. D., Fitzgerald, M., Eddy, W. F., Mintun, M. A., and Noll, D. C. (1995). Improved assessment of significant activation in functional magnetic resonance imaging (fMRI)—Use of a cluster-size threshold. *Magnetic Resonance Medicine*, *33*, 636–647.

Fox, P. T., and Raichle, M. E. (1986). Focal physiological uncoupling of cerebral blood flow and oxidative metabolism during somatosensory stimulation in humans. *Proceedings of the National Academy of the Sciences, USA*, *83*, 1140–1144.

Frahm, J., Bruhn, H., Merboldt, K.-D., Hanicke, W., and Math, D. (1992). Dynamic MR imaging of human brain oxygenation during restand photic stimulation. *JMRI: Journal of Magnetic Resonance Imaging*, *2*, 501–505.

Frank, L. R., Buxton, R. B., and Wong, E. C. (2001). Estimation of respiration—induced noise fluctuations from under sampled multislice fMRI data. *Magnetic Resonance in Medicine*, *45*, 635–644.

Friston, K. J., Holmes, A. P., Poline, J. B., Grasby, P. J., Williams, S. C., Frackowiak, R. S., and Turner, R. (1995). Analysis of fMRI time-series revisited. *NeuroImage*, *2*, 45–53.

Friston, K. J., Holmes, A. P., Price, C. J., Buchel, C., and Worsley, K. J. (1999). Multisubject fMRI studies and conjunction analyses. *NeuroImage*, *10*, 385–396.

Goldman, R., Stern, J., Engel, J., and Cohen, M. (2001). Tomographic mapping of alpha rhythm using simultaneous EEG/fMRI. *NeuroImage*, *13*, S1291–S1291.

Goodyear, B. G., and Menon, R. S. (2001). Brief visual stimulation allows mapping of ocular dominance in visual cortex using fMRI. *Human Brain Mapping*, *14*, 210–217.

Grinvald, A., Slovin, H., and Vanzetta, I. (2000). Non-invasive visualization of cortical columns by fMRI. *Nature Neuroscience*, *3*, 105–107.

Guimaraes, A. R., Melcher, J. R., Talavage, T. M., Baker, J. R., Ledden, P., Rosen, B. R., Kiang, N. Y. S., Fullerton, B. C., and Weisskoff, R. M. (1998). Imaging subcortical activity in humans. *Human Brain Mapping*, *6*, 33–41.

Gusnard, D. A., Akbudak, E., Shulman, G. L., and Raichle, M. E. (2001). Medial prefrontal cortex and self-referential mental activity: Relation to a default mode of brain function. *Proceedings of the National Academy of Sciences, USA*, *98*, 4259–4264.

Hasson, U., Nir, Y., Levy, I., Fuhrmann, G., and Malach, R. (2004). Intersubject synchronization of cortical activity during natural vision. *Science*, *303*, 1634–1640.

Haxby, J. V., Gobbini, M. I., Furey, M. L., Ishai, A., Schouten, J. L., and Pietrini, P. (2001). Distributed and overlapping representations of faces and objects in ventral temporal cortex. *Science*, *293*, 2425–2430.

Haxby, J. V., Hoffman, E. A., and Gobbini, M. I. (2000). The distributed human neural system for face perception. *Trends in Cognitive Science*, *4*, 223–233.

Hennig, J., Janz, C., Speck, O., and Ernst, T. (1997). Is there a different type of MR-contrast in early phases of functional activation. In *Advances in experimental medicine and biology*, vol. 413, pp. 35–42. Optical Imaging of Brain Function and Metabolism II. New York: Plenum Press.

Henson, R. N. A., Price, C. J., Rugg, M. D., Turner, R., and Friston, K. J. (2002). Detecting latency differences in event-related BOLD responses: Application to words versus non-words and initial versus repeated face presentations. *NeuroImage*, *15*, 83–97.

Hoge, R. D., Atkinson, J., Gill, B., Crelier, G. R., Marrett, S., and Pike, G. B. (1999). Linear coupling between cerebral blood flow and oxygen consumption in activated human cortex. *Proceedings of the National Academy of Sciences, USA*, *96*, 9403–9408.

Hopfinger, J. B., Buonocore, M. H., and Mangun, G. R. (2000). The neural mechanisms of top-down attentional control. *Nature Neuroscience*, *3*, 284–291.

Horovitz, S. G., Skudlarski, P., and Gore, J. C. (2002). Correlations and dissociations between BOLD signal and P300 amplitude in an auditory odd ball task: A parametric approach to combining fMRI and ERP. *Magnetic Resonance Imaging*, *20*, 319–325.

Hu, X. P., Le, T. H., and Ugurbil, K. (1997). Evaluation of the early response in fMRI in individual subjects using short stimulus duration. *Magnetic Resonance in Medicine*, *37*, 877–884.

Huettel, S. A., McKeown, M. J., Song, A. W., Hart, S., Spencer, D. D., Allison, T., and McCarthy, G. (2004). Linking hemodynamic and electrophysiological measures of brain activity: Evidence from functional MRI. *Cerebral Cortex*, *14*, 165–173.

Kanwisher, N., McDermott, J., and Chun, M. M. (1997). The fusiform face area: A module in human extrastriate cortex specialized for face perception. *Journal of Neuroscience*, *17*, 4302–4311.

Karni, A., Meyer, G., Jezzard, P., Adams, M. M., Turner, R., and Ungerleider, L. G. (1995). Functional MRI evidence for adult motor cortex plasticity during motor skill learning. *Nature*, *377*, 155–158.

Kelley, W. M., Miezin, F. M., McDermott, K. B., Buckner, R. L., Raichle, M. E., Cohen, N. J., Ollinger, J. M., Akbudak, E., Conturo, T. E., Snyder, A. Z., and Petersen, S. E. (1998). Hemispheric specialization in human dorsal frontal cortex and medial temporal lobe for verbal and nonverbal memory encoding. *Neuron*, *20*, 927–936.

Knight, D. C., Nguyen, H. T., and Bandettini, P. A. (2005). The role of the human amygdala in the production of conditioned fear. *NeuroImage*, *26*, 1193–1200.

Konn, D., Leach, S., Gowland, P., and Bowtell, R. (2004). Initial attempts at directly detecting alpha wave activity in the brain using MRI. *Magnetic Resonance Imaging*, *22*, 1413–1427.

Kwong, K. K., Belliveau, J. W., Chesler, D. A., Goldberg, I. E., Weisskoff, R. M., Poncelet, B. P., Kennedy, D. N., Hoppel, B. E., Cohen, M. S., Turner, R., Cheng, H. M., Brady, T. J., and Rosen, B. R. (1992). Dynamic magnetic resonance imaging of human brain activity during primary sensory stimulation. *Proceedings of the National Academy of Sciences, USA*, *89*, 5675–5679.

Laufs, H., Kleinschmidt, A., Beyerle, A., Eger, E., Salek-Haddadi, A., Preibisch, C., and Krakow, K. (2003a). EEG-correlated fMRI of human alpha activity. *NeuroImage*, *19*, 1463–1476.

Laufs, H., Krakow, K., Sterzer, P., Eger, E., Beyerle, A., Salek-Haddadi, A., and Kleinschmidt, A. (2003b). Electroencephalographic signatures of attentional and cognitive default modes in spontaneous brain activity fluctuations. *Proceedings of the National Academy of Sciences, USA*, *100*, 11053–11058.

Lemieux, L. (2004). Electroencephalography-correlated functional MR imaging studies of epileptic activity. *Neuroimaging Clinics of North America*, *14*, 487–506.

Levin, D. N., and Uftring, S. J. (2001). Detecting brain activation in fMRI data without prior knowledge of mental event timing. *NeuroImage*, *13*, 153–160.

Logothetis, N. K., Merkle, H., Augath, M., Trinath, T., and Ugurbil, K. (2002). Ultra-high-resolution fMRI in monkeys with implanted RF coils. *Neuron*, *35*, 227–242.

Logothetis, N. K., Pauls, J., Augath, M., Trinath, T., and Oeltermann, A. (2001). Neurophysiological investigation of the basis of the fMRI signal. *Nature*, *412*, 150–157.

Lomarev, M., Shastri, A., Ziemann, U., Wassermann, E. M., McConnell, K. A., Nahas, Z., Lorberbaum, J. P., Vincent, D. J., George, M. S., and Bohning, D. E. (2000). Can interleaved TMS and fMRI demonstrate changes in an activated circuit? In *Biological Psychiatry Annual Conference*, *47*, 97S (no. 323).

Lowe, M. J., Mock, B. J., and Sorenson, J. A. (1998). Functional connectivity in single and multislice echoplanar imaging using resting state fluctuations. *NeuroImage*, *7*, 119–132.

Lu, H. Z., Golay, X., Pekar, J. J., and van Zijll, P. C. M. (2003). Functional magnetic resonance imaging based on changes in vascular space occupancy. *Magnetic Resonance in Medicine*, *50*, 263–274.

Malonek, D., and Grinvald, A. (1996). Interactions between electrical activity and cortical microcirculation revealed by imaging spectroscopy: Implications for functional brain mapping. *Science*, *272*, 551–554.

Martin, A., Wiggs, C. L., Ungerleider, L. G., and Haxby, J. V. (1996). Neural correlates of category-specific knowledge. *Nature*, *379*, 649–652.

Mathiesen, C., Caesar, K., Akgoren, N., and Lauritzen, M. (1998). Modification of activity-dependent increases of cerebral blood flow by excitatory synaptic activity and spikes in rat cerebellar cortex. *Journal of Physiology*, *512*, 555–566.

McCarthy, G., Luby, M., Gore, J., and Goldman-Rakic, P. (1997). Infrequent events transiently activate human prefrontal and parietal cortex as measured by functional MRI. *Journal of Neurophysiology*, *77*, 1630–1634.

Menon, R. S. (2002). Post-acquisition suppression of large-vessel BOLD signals in high-resolution fMRI. *Magnetic Resonance in Medicine*, *47*, 1–9.

Menon, R. S., Luknowsky, D. C., and Gati, J. S. (1998). Mental chronometry using latency-resolved functional magnetic resonance imaging. *Proceedings of the National Academy of Sciences, USA*, *95*, 10902–10907.

Menon, R. S., Ogawa, S., Strupp, J. P., and Ugurbil, K. (1997). Ocular dominance in human V1 demonstrated by functional magnetic resonance imaging. *Journal of Neurophysiology*, *77*, 2780–2787.

Menon, R. S., Ogawa, S., and Ugurbil, K. (1995). High-temporal-resolution studies of the human primary visual cortex at 4T: Teasing out the oxygenation contribution in fMRI. *International Journal of Imaging Systems and Technology*, *6*, 209–215.

Noll, D. C., Genovese, C. R., Vazquez, A. L., O'Brien, J. L., and Eddy, W. F. (1998). Evaluation of respiratory artifact correction techniques in functional MRI using receiver operator characteristic analysis. *Magnetic Resonance in Medicine*, *40*, 633–639.

O'Doherty, J., Kringelbach, M. L., Rolls, E. T., Hornak, J., and Andrews, C. (2001). Abstract reward and punishment representations in the human orbitofrontal cortex. *Nature Neuroscience*, *4*, 95–102.

Ogawa, S., Lee, T. M., Kay, A. R., and Tank, D. W. (1990). Brain magnetic resonance imaging with contrast dependent on blood oxygenation. *Proceedings of the National Academy of Sciences, USA*, *87*, 9868–9872.

Ogawa, S., Lee, T. M., Stepnoski, R., Chen, W., Zhu, X. H., and Ugurbil, K. (2000). An approach to probe some neural systems interaction by functional MRI at neural time scale down to milliseconds. *Proceedings of the National Academy of Sciences, USA*, *97*, 11026–11031.

Ogawa, S., Menon, R. S., Tank, D. W., Kim, S. G., Merkle, H., Ellermann, J. M., and Ugurbil, K. (1993). Functional brain mapping by blood oxygenation level–dependent contrast magnetic resonance imaging: A comparison of signal characteristics with a biophysical model. *Biophysical Journal*, *64*, 803–812.

Ogawa, S., Tank, D. W., Menon, R., Ellermann, J. M., Kim, S. G., Merkle, H., and Ugurbil, K. (1992). Intrinsic signal changes accompanying sensory stimulation: Functional brain mapping with magnetic resonance imaging. *Proceedings of the National Academy of Sciences, USA*, *89*, 5951–5955.

Patterson, J. C., Ungerleider, L. G., and Bandettini, P. A. (2002). Task-independent functional brain activity correlation with skin conductance changes: An fMRI study. *NeuroImage*, *17*, 1797–1806.

Pellerin, L., and Magistretti, P. J. (1994). Glutamate uptake into astrocytes stimulates aerobic glycolysis—A mechanism coupling neuronal activity to glucose utilization. *Proceedings of the National Academy of Sciences*, *91*, 10625–10629.

Pessoa, L., Gutierrez, E., Bandettini, P. A., and Ungerleider, L. G. (2002). Neural correlates of visual working memory: fMRI amplitude predicts task performance. *Neuron*, *35*, 975–987.

Pfeuffer, J., Van de Moortele, P. F., Ugurbil, K., Hu, X. P., and Glover, G. H. (2002a). IMPACT: Image-based physiological artifacts estimation and correction technique for functional MRI. *Magnetic Resonance in Medicine*, *47*, 344–353.

Pfeuffer, J., Van de Moortele, P. F., Yacoub, E., Shmuel, A., Adriany, G., Andersen, P., Merkle, H., Garwood, M., Ugurbil, K., and Hu, X. P. (2002b). Zoomed functional imaging in the human brain at 7 tesla with simultaneous high spatial and high temporal resolution. *NeuroImage*, *17*, 272–286.

Raichle, M. E., MacLeod, A. M., Snyder, A. Z., Powers, W. J., Gusnard, D. A., and Shulman, G. L. (2001). A default mode of brain function. *Proceedings of the National Academy of Sciences, USA*, *98*, 676–682.

Rao, S. M., Bandettini, P. A., Binder, J. R., Bobholz, J. A., Hammeke, T. A., Stein, E. A., and Hyde, J. S. (1996). Relationship between movement rate and functional magnetic resonance signal change in human primary motor cortex. *Journal of Cerebral Blood Flow and Metabolism*, *16*, 1250–1254.

Rao, S. M., Binder, J. R., Bandettini, P. A., Hammeke, T. A., Yetkin, F. Z., Jesmanowicz, A., Lisk, L. M., Morris, G. L., Mueller, W. M., Estkowski, L. D., et al. (1993). Functional magnetic resonance imaging of complex human movements. *Neurology*, *43*, 2311–2318.

Rosen, B. R., Belliveau, J. W., Aronen, H. J., Kennedy, D., Buchbinder, B. R., Fischman, A., Gruber, M., Glas, J., Weisskoff, R. M., Cohen, M. S., Hochberg, F. H., and Brady, T. J. (1991). Susceptibility contrast imaging of cerebral blood volume: Human experience. *Magnetic Resonance in Medicine*, *22*, 293–299.

Saad, Z. S., Reynolds, R. C., Argall, B., Japee, S., and Cox, R. W. (2004). An interface for surface based intra- and inter-subject analysis with AFNI. In *Proceedings of the 2004 IEEE International Symposium on Biomedical Imaging*, 1510–1513.

Sereno, M. I., Dale, A. M., Reppas, J. B., Kwong, K. K., Belliveau, J. W., Brady, T. J., Rosen, B. R., and Tootell, R. B. H. (1995). Borders of multiple visual areas in human revealed by functional magnetic resonance imaging. *Science*, *268*, 889–893.

Shastri, A., Lomarev, M. P., Nelson, S. J., George, M. S., Holzwarth, M. R., and Bohning, D. E. (2001). A low-cost system for monitoring skin conductance during functional MRI. *Journal of Magnetic Resonance Imaging*, *14*, 187–193.

Shaywitz, B. A., Shaywitz, S. E., Pugh, K. R., Constable, R. T., Skudlarski, P., Fulbright, R. K., Bronen, R. A., Fletcher, J. M., Shankweiler, D. P., Katz, L., et al. (1995). Sex differences in the functional organization of the brain for language. *Nature*, *373*, 607–609.

Shmuel, A., Yacoub, E., Pfeuffer, J., Van de Moortele, P. F., Adriany, G., Hu, X. P., and Ugurbil, K. (2002). Sustained negative BOLD, blood flow and oxygen consumption response and its coupling to the positive response in the human brain. *Neuron*, *36*, 1195–1210.

Singh, K. D., Barnes, G. R., Hillebrand, A., Forde, E. M. E., and Williams, A. L. (2002). Task-related changes in cortical synchronisation are spatially coincident with the haemodynamic response. *NeuroImage*, *16*, 103–114.

Thompson, J. K., Peterson, M. R., and Freeman, R. D. (2003). Single-neuron activity and tissue oxygenation in the cerebral cortex. *Science*, *299*, 1070–1072.

Thompson, J. K., Peterson, M. R., and Freeman, R. D. (2004). High-resolution neurometabolic coupling revealed by focal activation of visual neurons. *Nature Neuroscience*, *7*, 919–920.

Tootell, R. B. H., Reppas, J. B., Kwong, K. K., Malach, R., Born, R. T., Brady, T. J., Rosen, B. R., and Belliveau, J. W. (1995). Functional analysis of human Mt and related visual cortical areas using magnetic resonance imaging. *Journal of Neuroscience*, *15*, 3215–3230.

Turner, R., Le Bihan, D., Moonen, C. T. W., Despres, D., and Frank, J. (1991). Echo-planar time course MRI of cat brain oxygenation changes. *Magnetic Resonance in Medicine*, *22*, 159–166.

Van Essen, D. C., and Drury, H. A. (1997). Structural and functional analyses of human cerebral cortex using a surface-based atlas. *Journal of Neuroscience*, *17*, 7079–7102.

Vaughan, J. T., Garwood, M., Collins, C. M., Liu, W., DelaBarre, L., Adriany, G., Andersen, P., Merkle, H., Goebel, R., Smith, M. B., and Ugurbil, K. (2001). 7T vs. 4T: RF power, homogeneity, and signal to noise comparison in head images. *Magnetic Resonance in Medicine*, *46*, 24–30.

Villringer, A. (1997). Functional neuroimaging. Optical approaches. *Advances in Experimental Medicine and Biology*, *413*, 1–18.

Visscher, K. M., Miezin, F. M., Kelly, J. E., Buckner, R. L., Donaldson, D. I., McAvoy, M. P., Bhalodia, V. M., and Petersen, S. E. (2003). Mixed blocked/event-related designs separate transient and sustained activity in fMRI. *NeuroImage*, *19*, 1694–1708.

Wagner, A. D., Schacter, D. L., Rotte, M., Koutstaal, W., Maril, A., Dale, A. M., Rosen, B. R., and Buckner, R. L. (1998). Building memories: Remembering and forgetting verbal experiences as predicted by brain activity. *Science*, *281*, 1188–1191.

Weiskopf, N., Veit, R., Erb, M., Mathiak, K., Grodd, W., Goebel, R., and Birbaumer, N. (2003). Physiological self-regulation of regional brain activity using real-time functional magnetic resonance imaging (fMRI). *NeuroImage*, *19*, 577–586.

Whalen, P. J., Rauch, S. L., Etcoff, N. L., McInerney, S. C., Lee, M. B., and Jenike, M. A. (1998). Masked presentations of emotional facial expressions modulate amygdala activity without explicit knowledge. *Journal of Neuroscience*, *18*, 411–418.

Williams, D. S., Detre, J. A., Leigh, J. S., and Koretsky, A. P. (1992). Magnetic resonance imaging of perfusion using spin inversion of arterial water. *Proceedings of the National Academy of Sciences, USA*, *89*, 212–216.

Williams, L. M., Brammer, M. J., Skerrett, D., Gordan, E., Rennie, C., Kozek, K., Olivieri, G., and Peduto, T. (2000). The neural correlates of orienting: An integration of fMRI and skin conductance orienting. *NeuroReport*, *11*, 3011–3015.

Windischberger, C., Langenberger, H., Sycha, T., Tschernko, E. A., Fuchsjäger-Mayerl, G., Schmetterer, L., and Moser, E. (2002). On the origin of respiratory artifacts in BOLD-EPI of the human brain. *Magnetic Resonance Imaging*, *20*, 575–582.

Wise, R. G., Ide, K., Poulin, M. J., and Tracey, I. (2004). Resting fluctuations in arterial carbon dioxide induce significant low-frequency variations in BOLD signal. *NeuroImage*, *21*, 1652–1664.

Wong, E. C., Buxton, R. B., and Frank, L. R. (1999). Quantitative perfusion imaging using arterial spin labeling. *Neuroimaging Clinics of North America*, *9*, 333–342.

Worsley, K. J., and Friston, K. J. (1995). Analysis of FMRI time-series revisited—Again. *NeuroImage*, *2*, 173–181.

Worsley, K. J., Marrett, S., Neelin, P., Vandal, A. C., Friston, K.J., and Evans, A. C. (1996). A unified statistical approach for determining significant signals in images of cerebral activation. *Human Brain Mapping*, *4*, 58–73.

Xiong, J. H., Gao, J. H., and Fox, P. T. (2003). Directly mapping magnetic field effects of neuronal activity by MRI. *Human Brain Mapping*, *20*, 41–49.

Yacoub, E., Shmuel, A., Pfeuffer, J., Van de Moortele, P. F., Adriany, G., Andersen, P., Vaughan, J. T., Merkle, H., Ugurbil, K., and Hu, X. P. (2001). Imaging brain function in humans at 7 tesla. *Magnetic Resonance in Medicine*, *45*, 588–594.